الجمهورية الجزائرية الديمقراطية الشعبية

**République Democratic and popular republic of Algeria**

وزارة التعليم العالي و البحث العلمي

**Ministry of Higher Education and Scientific Research**

جامعة وهران 2 محمد بن احمد

معهد الصيانة و الأمن الصناعي

**Institute of Maintenance and Industrial Safety**

**Electromechanical Department**

# MEMORY

In order to obtain the Master's degree

**Field:** Maintenance in Electromechanics

**Specialty:** Industrial Electromechanics

**Theme**

## *Parabolic-Through Concentrating Thermal Solar Power Plant*

Presented and publicly sustained by:

**YAHIAOUI Abdelaziz and ZENNANI Amran**

In front of the jury:

| First and last name | Grade | Establishment | Quality |
|---|---|---|---|
| **Mr. ACHACH Habib** | MCA | IMSI- University of Oran 2 | **President** |
| **Mr. DARRAMDANE MOHAMED ZOUHIR** | MCB | IMSI- University of Oran 2 | **Supervisor** |
| **Mr. BOUIADJRA Bachir** | MCB | IMSI- University of Oran 2 | **Examiner** |
| **Mr. SEDDAOUI Ali** | Doctoral st. | IMSI- University of Oran 2 | **Co-Supervisor** |

2022/2023

# THANKS

We thank Allah for all his countless blessings, and giving us willpower to begin and complete this work.

This work would not be as rich and would not have been possible without the great help and guidance of our teacher and supervisor **Mr. DARRAMDANE MOHAMED ZOUHIR.** We would like to thank him for his exceptional guidance, patience, discipline and availability during our study, our thanks to the chairman and members of the jury for examining and lending their interest to this work, special thanks to **Mr. SEDDAOUI Ali** who gave us important information about the parabolic-trough.

Our thanks also go to all our teachers for their generosity and great patience, despite their academic and professional responsibilities.

.

## Dedication

I would like to dedicate this work to my beloved ones, my entourage, my friends, family and especially my parents, whose unconditional support helped me to overcome the difficulties and moments of doubt inherent in this adventure. May they find, in the completion of this work, the culmination of their efforts and the expression of my most affectionate gratitude.

**YAHIAOUI Abdelaziz**

## Dedication

I thank God for helping us to accomplishing this work. I would like to dedicate this work to my family, friends, and especially my parents, who have been my support throughout my studies. I also thank the supervisor professor for helping us complete this work.

**ZENNANI Amran**

## Abstract

The main objective of this work is to simulate the thermal and dynamic behavior of a daily thermal energy storage system in solar thermal power plants.

Using the finite difference method and explicit scheme, the transient conduction equation is solved.

The heat storage battery is a Concrete pillar contain tubes, heat transfer fluid (liquid-sodium) leaves the parabolic trough concentrator then enters the battery forming a closed loop.

Optimization of battery is done by Modde 5.0 software. Input temperature is function of time and the results from the parabolic trough concentrator based in Ghardaia are used. The optimum parameters for the battery such as spacing between tubes, diameter and the heat transfer fluid velocity are 0.121m, 0.143m and 0.01m/s.



**Keyword**: Thermal energy storage, Numerical simulation, Sensible heat, Finite Difference Method, Modde 5.0 software.



## ملخص

الهدف الرئيسي من هذا البحث هو إجراء محاكاة عددية للسلوك الحراري والديناميكي لأنظمة تخزين الطاقة الحرارية اليومية في محطات الطاقة الشمسية الحرارية.

باستخدام طريقة الفروق المحدودة ، تم حل معادلة التوصيل الحراري المتغير بالنسبة للزمن.

بطارية تخزين الحرارة عبارة عن عمود خرساني يحتوي على أنابيب. السائل الناقل للحرارة (الصوديوم السائل) الخارج من مُجَمِّع الطاقة الشمسية المركزة يدخل البطارية و يعبر من خلالها لتشكل دورة مغلقة.

بمساعدة برنامج MODDE 5.0 وباستخدام نتائج المحاكاة العددية تمكنا من تحديد المعالم المثلى للبطارية مثل المسافة بين الأنابيب والقطر وسرعة الناقل الحراري للسوائل.

أظهرت النتائج أن المسافة المثلى بين الأنابيب هي0.121 متر, وقطر 0.143 متر, وسرعة الناقل الحراري 0.01 متر على الثانية.



الكلمات المفتاحية: تخزين الطاقة الحرارية، المحاكاة العددية، الحرارة المحسوسة، طريقة الفروق المحدود، برنامج Modde 5.0

# Summray

## Nomenclature

| | | |
|---|---|---|
| **T** | Temperature | **°C** |
| **t** | Time | **s** |
| **Q** | Heat quantity | **J** |
| **A** | Area | **$m^2$** |
| **D** | Diameter | **m** |
| **L** | Length | **m** |
| **W** | Width | **m** |
| **Cp** | Heat capacity | **$J/Kg \cdot K$** |
| **h** | Convection coefficient | **$W/m^2 \cdot C$** |
| **V** | fluid velocity | **m/s** |
| **S** | the surface area | **$m^2$** |
| **k** | Thermal conductivity | **$W/K.m$** |
| **I** | The incident solar radiation | **$W/m^2$** |
| $\dot{m}$ | Mass flow | **Kg/s** |
| $h$ | Enthalpy | **J/kg** |

| | | |
|---|---|---|
| $\dot{Q}_e$ | Power radiated | **W** |
| $\sigma$ | The constant of Stefan Boltzmann | **$W/m^2.K^4$** |
| Q | Heat quantity | **J** |
| **E** | Energy | **J** |

- **Greek Symbols**

| | | |
|---|---|---|
| $\boldsymbol{\alpha}$ | Thermal diffusivity | **$m^2.s$** |
| $\boldsymbol{\rho}$ | Density | **$Kg/m^3$** |
| $\boldsymbol{\varphi}$ | Heat flow | **W** |
| $\boldsymbol{\mu}$ | Dynamic viscosity | **Pa.s** |
| $\boldsymbol{\varepsilon}$ | Surface emissivity | |

- **Subscripts**

| | |
|---|---|
| He | Heat exchanger |
| Hf | Heat fluid |
| T | Total |
| Re | Release |
| F | Fluid |
| V | Vapor |

- **Dimensionless Numbers**

| | |
|---|---|
| **Gr** | Grashof number |
| **Re** | Reynolds number |
| **Pr** | Prandtl number |
| **Nu** | Nusselt number |
| **F0** | Fourrier number |

**Bi** Biot number

$\eta$ Efficiency

- **List of Abbreviations**

**CSP** Concentrated Solar Power.

**PTC** Parabolic trough collectors.

**STEM** Sensible thermal energy storage materials.

**HTF** Heat transfer fluid.

**SEGS** Solar electric generating systems.

**TES** Thermal energy storage.

**SCAs** Solar collector assemblies.

**HCE** Heat Collection Elements.

**PCM** Phase Change Materials.

**FDM** Finite difference method.

**PDE** Partial differential equation.

- **Indices**

**I** Index of a subsequent mesh point x

**J** Index of a mesh point following y

**S** Solid

**F** Fluid

**T** Time to initial condition

**I** Inlet

**E** Exit

**W** Average of input and output

- **Mathematical Operators**

| | |
|---|---|
| $\boldsymbol{\Delta}$ | Variation |
| $\boldsymbol{\partial}$ | Partial derivative |
| $\frac{\boldsymbol{d}}{\boldsymbol{dt}}$ | Derivative with respect to time |
| $\frac{\boldsymbol{d}}{\boldsymbol{dx}}$ | Derivative with respect to space |
| $\frac{\boldsymbol{\partial}}{\boldsymbol{\partial x}}$ | Partial derivative with respect to space |
| $\frac{\boldsymbol{\partial}}{\boldsymbol{\partial t}}$ | Partial derivative with respect to time |

# Figures List

## Table List:

# Introduction

## General Introduction

In order to protect our environment, our world needs to reduce $CO_2$ emissions. The recourse to photovoltaic power plants "PV" causes a sharp drop in the yield of electricity production with the increase of temperature, which is not a practical solution in the hot climate regions.

The technology of concentrated solar power (CSP) concentrators has just reached a very advanced level, so the solar power plants are more profitable in hot countries like North Africa.

Thermal energy storage is a crucial component of CSP systems. It allows for the capture and storage of excess heat generated during peak sunlight hours, which can then be utilized to generate electricity during periods of low or no sunlight. This storage capability enables CSP plants to provide power even when the sun is not shining, making them a more reliable and consistent renewable energy option.

Parabolic trough concentrated solar power (CSP) is one of the most established and widely used technologies within the CSP industry. It utilizes parabolic-shaped mirrors, known as troughs, to concentrate sunlight onto a receiver tube located at the focal point of the parabola.

In the first chapter, the work done on the thermal energy storage (sensible) and the parabolic trough thermal concentrated solar power plant is presented.

In the second chapter, the operations principle and theoretical study for Parabolic- trough collectors and thermal energy storage is shown.

In the third chapter, the studied case is explained. In the fourth chapter, the main results are discussed.

# Chapter I

# Review of Literature

## I.1. Introduction

Parabolic trough solar thermal power plants are a type of concentrated solar power (CSP) system that uses parabolic mirrors to concentrate sunlight onto a receiver tube. The heat from the receiver tube is then used to generate steam, which drives a turbine to generate electricity.

Sensible heat storage is a type of thermal energy storage that uses a material that can store heat by changing its temperature. In a parabolic trough CSP system, sensible heat storage is used to store the heat from the receiver tube during periods of low sunlight, such as at night or during cloudy weather. This stored heat can then be used to generate electricity when the sun is not shining.

In recent years, significant work has been done to modernize the technology of parabolic trough and sensible heat storage CSP systems. The focus of this work was on improving system performance, reducing system costs and increasing system reliability.

Thanks to these advances, parabolic CSP systems are one of the most competitive renewable energy technologies available today. They are a reliable and efficient way to generate electricity from the sun. Also, sensible heat storage is now a mature and reliable technology capable of storing heat from a variety of sources, including solar power plants, industrial processes and even wastes heat. Sensible thermal storage is a key component of many renewable energy systems and environmentally friendly.

## I.2. Concentrated Solar Power Technology

One of the most promising technologies to replace current fossil fuel-based and nuclear power facilities is concentrated solar power [18]. It is built on reflectors that can monitor the sun throughout the day to capture the highest solar flux at the focus system. These reflectors redirect and concentrate solar irradiance into a receiver. In order to create electricity, the solar energy that has been captured is transported as heat to the power system's heat transfer fluid (HTF). Due to the ability of the plants to provide base load support through hybridization or assimilation of TES system, interest in concentrating solar power technologies has been developing significantly.

Through a shared power cycle, the hybrid technology frequently allows CSP plants and conventional power plants to operate in parallel [19]. The first hybridization method is regarded as the most advanced solar-hybrid technology to overcome the intermittent nature of solar

energy. Other hybridization methods include the use of fossil fuel backup systems, coal-fired power plants, and combined cycle plants. A commercial and significant installation of solar electric generating systems (SEGS) plants has used a fuel backup system [20]. The TES system in CSP facilities, on the other hand, functions as a component that stores produced thermal energy during periods of high solar irradiation. It has been demonstrated to be a trustworthy method for increasing the capacity of CSP plants [21], extending the production window when there is not enough.

## I.3. The Work Carried out on Parabolic Trough

The work carried out on a parabolic trough solar collector is to concentrate sunlight onto a receiver tube, which heats up a fluid inside the tube. The heated fluid is then used to generate electricity or process heat.

The parabolic trough collector is made up of a long, trough-shaped mirror that is parabolic in cross-section. The mirror is mounted on a tracker that follows the sun across the sky. The receiver tube is positioned at the focal point of the parabola, so that the concentrated sunlight is focused directly onto the tube.

The fluid inside the receiver tube can be water, synthetic oil, or molten salt. The type of fluid used depends on the application. Water is typically used for low-temperature applications, such as domestic hot water heating. Synthetic oil and molten salt are used for high-temperature applications, such as electricity generation.

The heated fluid from the receiver tube is then used to generate electricity or process heat. For electricity generation, the heated fluid is used to drive a steam turbine, which generates electricity. For process heat applications, the heated fluid is used directly in the industrial process. [1]

When compared to other solar power designs on the market, parabolic trough technology is thought to be the most developed. It has been used by numerous large-scale CSP plant operations all around the world. The first installation, which took place thirty years ago, continues to be the biggest commercial use of the parabolic trough system today. The first Solar Electric Generating Systems (SEGS) plant, with a 354 MW capacity, was built in 1984 [22]. The first plant (SEGS-I), followed by the remaining eight power plants, started operating in 1985. The final unit (SEGS-IX), started operating in 1991 [23].

It has nine power plant facilities and more than two million square meters of parabolic trough collectors distributed throughout the Mojave Desert in southern California [23]. These plants use synthetic heat transfer oil that is heated by captured solar irradiance and circulated across the solar field to circulate in the receiver tubes. Additionally, the use of solar energy through parabolic trough CSP plants accounts for approximately 1220 MWe of installed power globally, distributed among 29 operational plants, the majority of which are located in Spain and the United States [24].

## I.4. The Work Carried out on the Sensible Heat Storage

### I.4.1. Water Tank Storage

Water tank storage is the most well-known and most commonly used technology. It can be used for seasonal and daytime applications, although the size of the seasonal storage tank is very large and is therefore not economical. The choice of the tank and the insulation materials are the main factors that influence the efficiency and the cost of the tank [2]

**Sergii Bespalko** et **al**. gave an overview of the existing sensible heat storage technologies applied in thermal energy systems based on fluctuating renewable heat sources to overcome the problem of mismatch between the supply and consumption of thermal energy.

They discovered that sensitive storage substances cannot provide constant temperatures during charging and discharging; therefore, to store more heat, greater overheating is necessary, which leads to essential heat losses and a reduction in storage efficiency. [3]

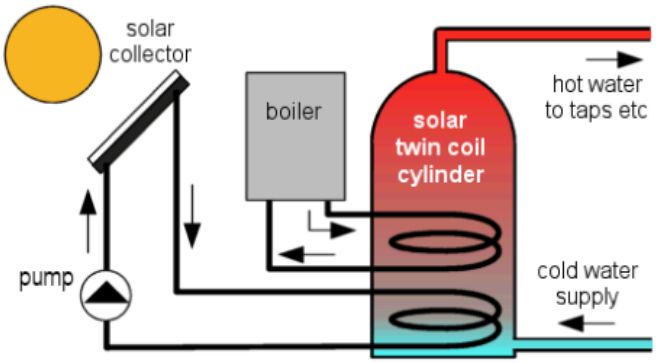


Figure I- 1: Solar hot water supply system.

Figure I- 1 shows diagram of the solar hot water supply system with a hot water storage tank.

Using solid graphite materials for water heating was proposed by **Chengyao Guan** et **al**. The results showed that the standard deviation of the outlet temperature was reduced by 68.49% and 68.81% for one- and two-tank systems. [4]

For the request change condition, the control strategy was performed on the basis of the criterion of thermal power balance in both heat exchangers. The result showed that the single tank will lead to negative initial effects on the quality of the water heating, although it can stabilize the oscillation of the temperature output.

For the dual-tank system, a two-step adjustment method has been applied. State-of-the-art projects have shown that water storage in a tank is a cost-effective storage option and that its efficiency can be further improved by ensuring optimal stratification of the water in the tank and thermal insulation very effective. [5]

### I.4.2. Packed Bed Storage

A packed bed storage unit (pebble bed) uses the capacity of the material weakly packed particulate to store energy. A fluid, usually air, circulates in the bed to add or remove widely used materials. In operation, the flow is maintained through the bed in one direction during the addition of heat (generally downwards) and in the other direction of heat elimination. [5]

The first analytical study was carried out by **Schuman** [6], and the basic hypotheses leading to this model are a one-dimensional flow, no conduction or axial dispersion, constant properties, no mass transfer, no heat loss in the environment and no temperature gradients within the solid particles.

**Rayan Anderson** et **al**. [7] examined an approach to an equation for the storage of thermal energy in a bed lined with alumina with area as a heat transfer fluid. This modeling approach assumes a thermal equilibrium between the fluid and solid phases. The model solves the axial and radial temperature profiles in the lined bed, the insulation and the tank.

The study by **Panna Lal Singh** et **al**. [8] indicated that the fixed-bed solar heat storage system was suitable for storing the heat of solar area heaters. The temperature gain in the packed bed was significantly affected by solar radiation. The temperature of the packed bed has increased from 34°C to 49°C during the charging mode.

**Magdalena Nems** et **al.** [9] present the results of a study on a lined bed filled with ceramic bricks. The designed storage facility is supposed to be part of a heating system installed in a single-family house and possibly be integrated with a concentrated solar collector. The choice of ceramic bricks as a filling material was dictated by several reasons

- Structural stability.
- Good thermal properties.
- Resistant to high temperatures.
- Does not emit any harmful gases.

As Wothing is demonstrated in [9], a system in which the heat is stored in a sensible heat storage material, such as ceramic brick, must be provided with a means of controlling the flow in order to maximize the efficiency of the heat storage process, if the heat comes from a source of variable intensity, such as a concentrated air solar collector.

### I.4.3. Thermal Energy Storage

A major complication of using solar energy is the erratic availability of the source, resulting in unbalanced production during the day and even year-round. In CSP plants, thermal energy storage (TES) has many functions. Balance the plant in changing weather conditions. For example, when clouds cover the sky over a solar power plant site, it can cause a temporary change in the fluctuation of the incoming solar flux. As a result, the operation of the turbine can be significantly impaired by the change in operation with a significant drop in this case; the integration of a heat accumulator can ensure the stability of the turbine through base-load operation. In addition, TEST can store solar energy collected during the day and convert it into electricity in a power plant. It allows you to feed electricity into the grid during consecutive peak periods.

The basic requirements for thermal energy storage systems for a CSP depend on several parameters, including charge and discharge heat rates, power capacity, reasonable or latent heat storage, maximum and minimum temperatures, thermal and chemical stability of the number of cycles, heat loss [27]. The most widely used thermal energy storage in CSP facilities is a double-tank thermal storage system that uses molten salt as a thermal storage medium. It is the most advanced technology for both parabolic trough and solar tower power systems. Unlike the solar tower system, which has a double-tank direct system in which molten salt is used as a heat transfer liquid and storage medium, thermal energy storage is used as an indirect system in a parabolic trough solar power plant because it mainly uses thermal oil as heat absorption liquid.

### I.4.4. Other Works in the Field

**Yongfang Jian** et **al.** [10] used a one-dimensional to describe the thermal behavior of a solid heat storage module. Optimized solid storage module designs have been provided for various system requirements. The optimized results indicated that the inner diameter of the heat transfer tube should be 16mm.

**Abdul Jabbar** et **al.** [11] conducted a numerical study of the thermal behavior of solar walls. Three different storage materials were examined, namely concrete, hydrated salt and paraffin. The optimal thickness of 8cm is defined as the hydrated salt wall capable of maintaining a comfortable temperature in the region of fluctuations in ambient temperature.

The study by **Messaoud Sandali** et **al.** [12] shows an improvement in thermal behavior, especially after noon. With the integration of the porous medium, the temperature of the drying area increases by 4°C and extends the operation of the solar dryer by two hours after sunset. The increase in the thickness of the pores lengthens the residence time of the drying air inside the porous medium.

Through a 3D numerical analysis, **Prasad** et **al.** [13] examined the transient behavior and storage capacity of sensitive heat storage cells for thermal storage in a temperature range of 523 to 673K. Three materials are used for storage, concrete, steel and cast iron. The storage efficiency of the three materials was evaluated the main result of the study.

**Burcu Koçak** et **al.** [14] have attempted to examine these latest trends in sensitive thermal energy storage systems and materials used in industrial solar applications. The objective is to provide information for the continuation of research and development that will make solar heat a cost-effective method to meet the growing energy needs of the industrial sector. And they ended up finding that

- There is an urgent need in the industry to switch from fossil fuel-based energy systems to renewable energy sources. Solar energy is the most abundant and promising source of renewable energy, but it has not yet been widely used in industrial applications.
- Industrial solar heating processes are classified into 3 groups according to a temperature range: low temperature (below 150°C), medium temperature (150-400°C) and high temperature (above 400°C). Current industrial solar applications are generally intended for low process temperatures due to the availability of low-cost solutions by flat sensors.
- Latent and thermochemical heat storage systems have higher energy densities than sensitive heat storage systems, but for medium to high temperature industrial

applications, cost-effective solutions can only be obtained with sensitive heat storage systems.

- Sensible thermal energy storage materials (STESM) such as rock, sand or soil are well-known and abundant natural materials used for a medium to high temperature range. The need for thousands of tons of STESM in industrial applications may not be a sustainable solution due to the significant depletion of natural sources.
- Waste-based materials such as STESM show promise for high-temperature TES applications up to 1000°C. STESM increase the durability of solar heat applications in industry by reducing greenhouse gases and intrinsic emissions and reducing costs. They have good thermal properties with high thermal stability, heat capacity and thermal conductivity.

## I.5. The Work that Has Been Carried out in our Institute

The work that was done by **Chekaba. A** and **Bougera. A** [15] results in a numerical simulation of the thermal and dynamic behavior of a sensible daily thermal energy storage system in an installation. The finite difference method is used for solving the unsteady conduction equation with a one-dimensional model and an implicit scheme.

In this study, the effects of the velocity of the heat transfer fluid, the temperature distribution and the heat transfer in solid storage media are presented for different materials. This study allowed them to predict and estimate the number of storage modules that drive the steam turbines of solar thermal power plants.

The numerical results of this study demonstrate that the technology of high temperature heat storage in concrete is an attractive technology in the industrial field.

In the previous study on the subject, **Koumad. A** and **Chiad. F** [16] concluded with a work on a solar thermodynamic device; that in this two-dimensional model, the resolution of the unsteady conduction equation is carried out using the finite differences method of implicit form. And by choosing a speed of the heat transfer fluid of 0.06m /s and a distance between the tubes of 50 cm, the results of the calculations show that the concrete has good performance compared to other configurations. In addition, the method they chose to solve the Gauss matrix could not lead to a concrete result.

**Rahal**. **A** and **Khalifa med**. **A** [17] simulate 2D model, using the finite difference method and an explicit scheme.

In their study, they investigated the effect of the velocity of the liquid on the temperature distribution in both the storage and release cycle, taking into account the change in the temperature of the liquid through the thermal battery. They decided to choose a fluid velocity at the storage stage of 0.5 m/s and for the release a velocity of 0.01 m/s, a diameter of 1 cm, a pipe spacing of 30 cm and a battery length of 10 meters.

They chose concrete because it is easy to handle, the main aggregates are available all over the world, there are no ecologically vital components. It also showed good performance in terms of heat capacity compared to other solids

In the current work, we will solve a two-dimensional model of heat diffusion as a function of time using an explicit finite difference scheme, unlike the previous studies the temperature of the input liquid changes every 10 minutes , this temperature is set according to parabolic trough collector simulations.

## I.6. Conclusion

In this chapter, the work done on the thermal energy storage (sensible) and the parabolic trough thermal concentrated solar power plant was presented.

The next chapter contains the theoretical study.

# Chapter II

# Theoretical Study

## II.1. Introduction

Concentrated solar energy and thermal energy storage are promising innovative technologies for the generation of clean and sustainable energy. Concentrated solar energy systems use mirrors or lenses to focus sunlight onto a receiver, converting solar radiation into thermal energy. This thermal energy can be used for a variety of applications, including power generation, heating, and industrial processes. To ensure continuity of energy supply, thermal energy storage systems store excess thermal energy for later use during periods of high solar radiation when sunlight is not available.

Thermal energy storage system is an important part of concentrating solar energy systems. These storage systems capture excess thermal energy during times of strong solar radiation and store it for later use. Stored energy can be released when needed, allowing power generation to continue even when solar power is unavailable. Thermal energy storage technologies aim to optimize energy storage efficiency and capacity to ensure a reliable and constant energy supply.

The development of concentrated solar power and thermal energy storage technology is being driven by the growing demand for renewable energy sources and the need to reduce greenhouse gas emissions. These technologies offer a sustainable alternative to traditional fossil fuel generation and contribute to a cleaner and greener energy landscape. Ongoing research and advances in materials, storage media and system design continue to improve the efficiency and cost-effectiveness of concentrated solar power and energy storage systems, making them increasingly viable options for large-scale power generation.

In summary, concentrated solar power and thermal energy storage technologies represent a promising path towards a sustainable, low-carbon energy future. Harnessing the power of the sun and efficiently storing thermal energy, these technologies provide a reliable and clean source of electricity and heat. As research and development continues, concentrated solar power and thermal energy storage will play an important role in the transition to a more sustainable energy system.

## II.2. Concentrated Solar Power Technology

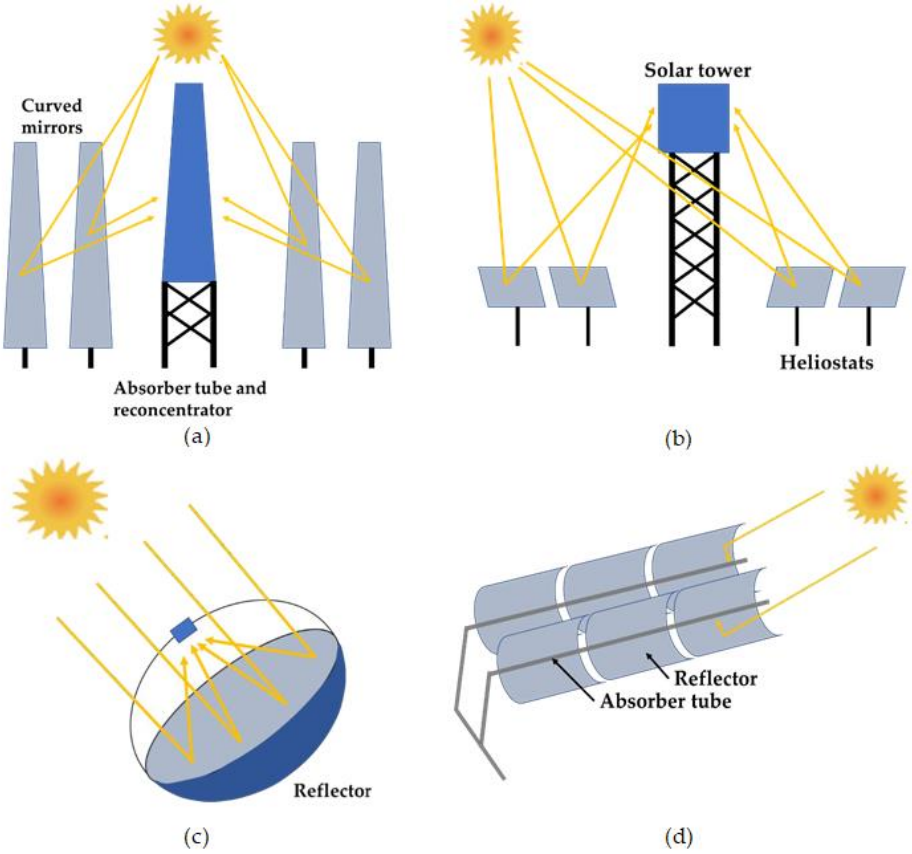


Figure II- 1: Types of collector technologies in CSP plant: Fresnel reflector (a), solar tower (b), parabolic dish (c) and parabolic trough (d), inspired by [25].

As depicted in figure II-1, there are four commercial CSP technologies: the linear Fresnel, the parabolic trough, the solar tower, and the parabolic dish. According to the process of sun-tracking and the concentrator focus geometry; there are two broad groups of solar gathering systems. The sun-tracking mechanism enables the solar collectors to make extensive use of solar irradiance over the course of a day. The first group includes single-axis sun-tracking systems, which track the sun's path across the horizon and focus direct solar irradiance onto a focal line inside a linear receiver [19]. This uses parabolic trough and linear Fresnel technology and is referred to as line focusing systems. The sun can be tracked along the two axes in the second category. A single point of receiver receives all of the irradiance that strikes collectors surfaces. Point focusing systems are made up of solar tower and parabolic dish technologies that are

arranged according to common principles. Two axis tracking helps the device achieve greater temperatures in the receiver aperture and increases the optical efficiency of the collectors [26].

Additionally, fixed or mobile assemble receiver criteria can be used to distinguish CSP technologies. An independent collector facet that is separate from the receiver exists in a fixed type receiver. A mobile type receiver, in contrast to that structure, is grouped with the collection and travels with it as a unit to pursue the sun [19]. The linear Fresnel reflector and solar tower fall within the fixed receiver group, whereas the other two reflector types are movable assemble receivers, as may be inferred from the aforementioned explanations. Each of these concentrators may function in a variety of temperature ranges and concentration ratios. In the following section, many CSP technology attributes are explained.

### II.2.1. Types of Concentrating Solar Technologies

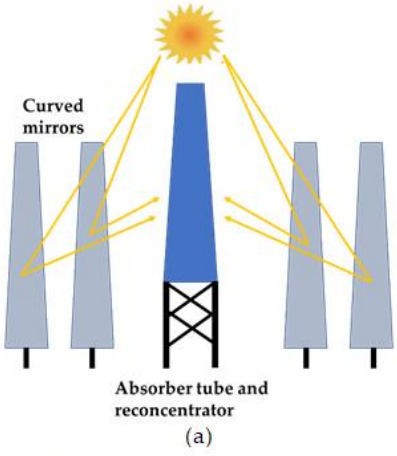


Figure II- 2: Fresnel reflector.

The first technology, Fresnel reflector shown in figure II-2, was firstly invented by **Augustin- Jean Fresnel**, a French-born physicist, for the function in lighthouses [27]. A wide commercial development of Fresnel reflectors, however, only began in 2009. It was when **Novatec Biosol**, the German manufacturing company, successfully supplied the Fresnel collectors to build up the solar field in CSP plant with 1.4 MW capacity of electrical production [22]. The general arrangement of linear Fresnel collectors is to align long arrays of flat mirror stripes horizontally to track the sun. These mirrors reflect the light onto a standalone linear receiver that is mounted on a tower which is usually constructed in between 10 to 15 m high [22].

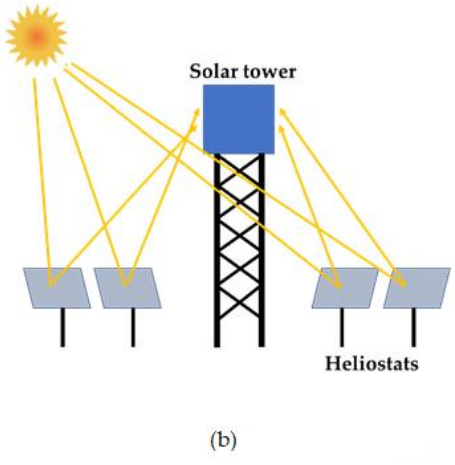


Figure II- 3: Solar tower.

Another technology, solar tower in figure II-3, is the most recent CSP technology to emerge commercially that comprises of heliostat collectors. The collectors are designed in large array of flat mirrors spread around the heat absorbing receiver located in the central of the solar field [22]. The receiver is located on top of the tower that is mounted to the ground and each heliostat lies on the two-axis tracking system.

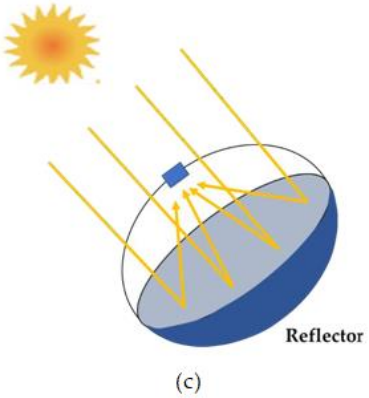


Figure II- 4: Parabolic dish collector.

Furthermore, as seen in figure II-4, parabolic dish collector is the two-axis tracking systems. It concentrates the solar radiations to the thermal receiver located on the focal point of the dish collector. Sunlight enters the collector area as the result of normal incidence. Parabolic dishes exploit only the sun direct normal irradiation.

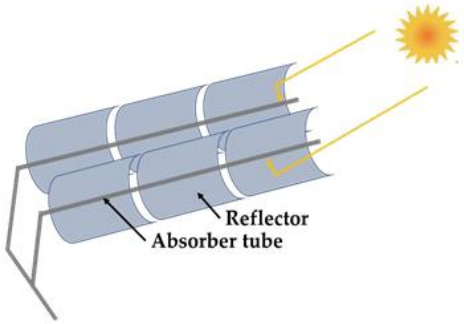


Figure II- 5: Parabolic trough solar collector.

The parabolic trough technology (PTC), which can be seen in figure II-5, is the fourth type of solar collector. It consists of reflective mirrors that have been parabolically bent and assembled to form a long trough that reflects the sun's direct irradiance onto a fluid-carrying receiver tube. Depicts the parabolic trough collector's component parts. The parabolic trough concentrator must be positioned correctly to take in and reflect solar energy onto the receiver tube as the sun's apparent location in the sky changes throughout the day. To change the concentrator's location during one-axis rotation.

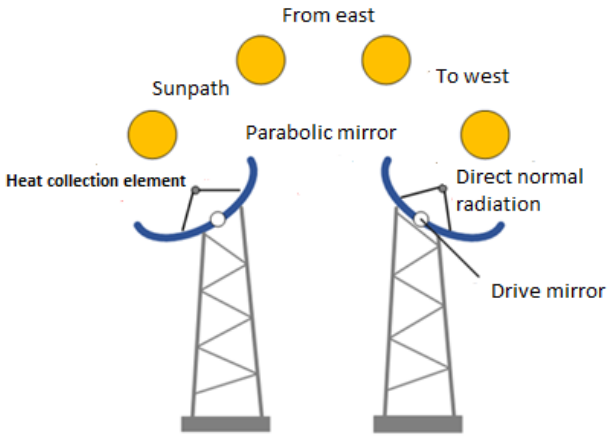


Figure II- 6: Trough with single-axis tracking, inspired by [28].

Parabolic trough collectors can be aligned either on east-west direction or north- south direction figure II-6; both orientations have been widely implemented in commercial parabolic trough CSP plants, with different considerations when taking the decision of orientation. Major aspects of deliberation are basically determined by the application of parabolic CSP plant which consequently links a linear correlation with the annual demand of energy. The north-south alignment follows the sun path from east to west and is reported to produce higher thermal energy. This literally means the alignment can maximize the annual energy output compared to east-west alignment, which tracks the sun from south to north. However, the installation of the parabolic troughs following the east-west alignment can benefit from the harvesting of solar energy at solar noon in winter season [22].

## II.3. Parabolic Trough CSP Plants

### II.3.1. Operating Principle:

The idea of a parabolic trough collector (PTC) is to focus sunlight onto a small area to generate high temperatures that can be applied to a variety of tasks, including the production of electricity.

A PTC is made up of a long reflector with a parabolic form that directs sunlight onto a receiver tube at the parabola's focal point. The reflector is often comprised of polished metal or glass mirrors and can pivot to follow the sun's path throughout the day.

A heat transfer fluid, like oil or molten salt, is heated by the concentrated sunlight inside the receiver tube. After being pumped into a heat exchanger, the hot fluid transmits its heat to a working fluid, usually water, where it is transformed into steam.

After that, the steam powers a turbine to produce energy.

A PTC must be pointed toward the sun and carefully placed to ensure that the reflected sunlight is perfectly concentrated on the receiver tube in order to operate as efficiently as possible. PTCs are made to be modular, and a solar field can be created by connecting many troughs together.

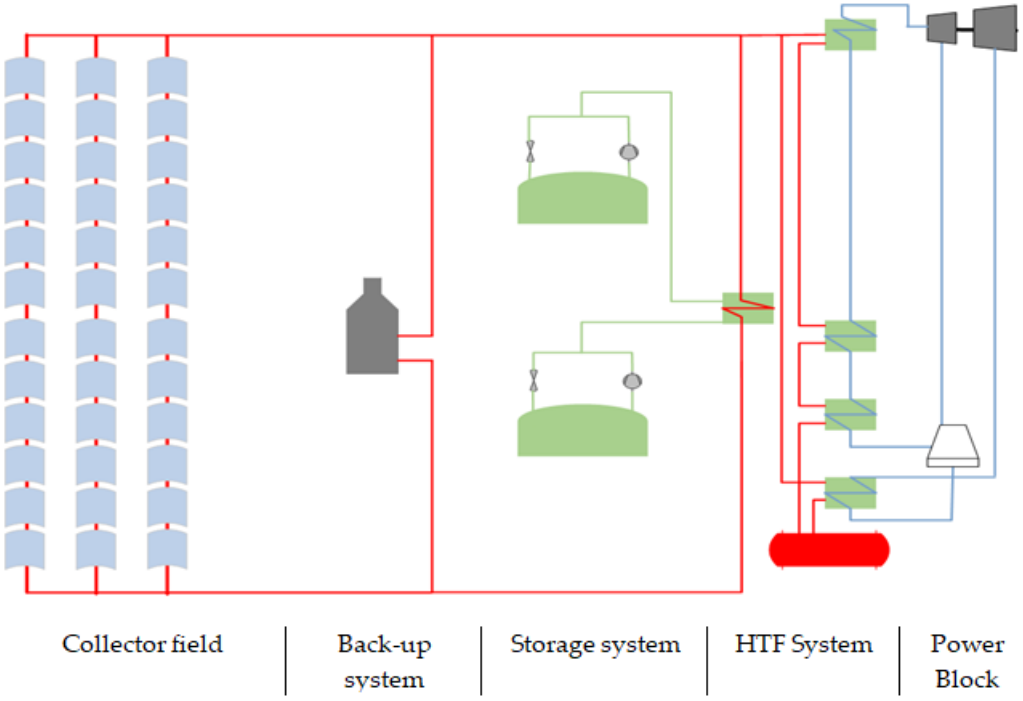


Figure II- 7: Parabolic trough plant scheme, inspired by [27].

The configuration of conventional parabolic-trough plants is depicted in figure II-7, which is primarily separated into the storage system, the power block, and three interconnected subsystems: the solar field.

In addition to these parts, some CSP plants may additionally incorporate a backup system made up of an auxiliary heater—the device situated between the solar field and the energy storage—that enables the plant to run even when solar radiation and the thermal energy in the storage are unavailable. In some facilities, the auxiliary heater may be situated inside the power block, allowing for the direct production of superheated steam for the steam turbine. Because this configuration lessens the likelihood of producing thermal losses in the oil circuit, it is predicted to provide higher overall plant efficiency than the solar field auxiliary heater [29].

### II.3.2. The Solar Field

The cornerstone of the parabolic trough system is the solar array, which consists of all components assembled together, with multiple solar collector assemblies (SCAs) connected to form one or more circuits, with each circuit arranged in parallel. Each SCAN consists of a series of in-line parabolic collector modules and heat recovery units (HCE) installed in the focal line of the parabolic surface. It is a block in which solar radiation is captured and converted into thermal

energy in the form of sensible heat, which is transported by a working fluid flowing through receiving pipes and a piping system to a storage or injection unit. Manifold circuits are connected to a cold manifold and a hot manifold, allowing antifreeze to flow into each circuit. One collector transports cold HTF for heating in a solar panel and another collector collects hot HTF for distribution to a power plant for power generation and/or thermal energy storage for later use in special circumstances.

### II.3.3. Back up

The backup system of a power plant with an equivalent sink includes redundancy in the main components and alternative energy sources to ensure continuous operation.

### II.3.4. Power Block

This subsystem converts the thermal energy supplied by a solar panel or storage system into electricity. This is done using a typical Rankin cycle, which consists of several components: pumps, cooling systems, steam turbine, power generator and water/steam heat exchangers. Typically, on a clear day, the solar array will receive a direct normal irradiance of 100 to 300 $w/m^2$ and the working fluid will circulate through the solar array until it reaches its nominal outlet temperature. [29]

Fluid transfers the thermal energy to another subsystem to store the thermal energy or to a steam generator to drive the turbine and power the power plant. In the summer months, the field receives a large amount of solar radiation, sufficient to keep the power plant at full load during the day and to recharge the thermal energy reserves. However, the thermal output of the solar field during the day on cloudless winter days is significantly lower than in summer, which is only sufficient for the operation of one power unit.

## II.4. Thermal Energy Storage

### II.4.1. Working Principle

The basic principle is the same in all thermal energy storage (TES) applications. The energy is supplied to a storage system to be withdrawn and used later. What varies is the scale of the storage and the storage method used.

A complete storage process involves at least three steps: Charging, storing and discharging. A simple storage cycle can be illustrated as in figure II-8. [30]

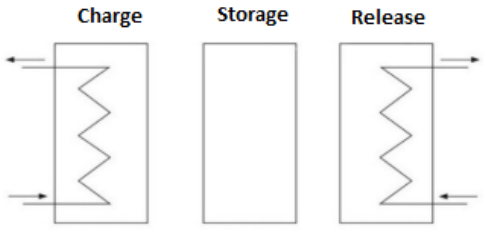


Figure II- 8: Storage cycle.

Thermal storage allows for a better use of renewable energy resources, for example in combination with heat production from solar thermal energy. It helps to reduce and compensate for peak loads in the energy demand. [31]

### II.4.2. Classification of TES According to the Storage Methods

Thermal energy storage has three basic methods

#### II.4.2.1. Sensible Heat Storage

The principle of a sensible thermal energy storage system is that solids and liquids experience temperature changes while storing and releasing thermal energy. This temperature change does not cause any further change, so sensible heat storage is considered a cost-effective storage system. In addition, a wide range of solid and liquid materials can be used in sensible heat storage. With a solid material, the heat transfer fluid flows inside the TES. The advantages of the system result from the process and the use of inexpensive solids as storage materials such as bricks and silicate concrete [22].However, it is believed that solids have a low thermal density, making the storage process inefficient [32].

Because of their high conductivity and heat capacity, liquid media, on the other hand, have been frequently used in sensible TES systems in the form of molten salts and oils [33]. Molten salts in particular have emerged as leaders in the use of thermal storage systems in CSP plants. This is due to the possibility of using the liquid not only as a storage medium, but also as a heat transfer liquid. In addition, the operating temperature of the molten salt is very ideal for high-temperature steam turbines in the power generation cycle. [26]

#### II.4.2.2. Latent Heat Storage

Latent thermal storage, the second category, warms the storage medium until it melts and forms another phase. The process occurs at a specific temperature and involves solid-liquid or liquid-vapor phase transitions. The storage medium that exhibits phase-change phenomena is often Phase Change Materials (PCM), with organic PCMs having been demonstrated to have a high energy density and excellent thermo-physical properties when compared to sensible heat storage materials. It benefits the system since the temperature during the phase transition can be used to control the system temperature as an approximate constant level. PCMs have a drawback in that they have limited thermal conductivity, which results in slow charge and discharge rates.

#### II.4.2.3. Thermo Chemical Heat Storage

In the thermo chemical heat storage, thermal energy forces the endothermic chemical reaction to form the chemical bonds. This occurs in the storage charge scheme at high temperatures. Meanwhile, during the storage discharge, the chemical bonds break down under an exothermic reaction and release thermal energy for electricity generation [22]. Thermochemical heat storage is seen to be compatible for higher temperatures compared to sensible and latent heat storages.

### II.4.3. Classification of TES According to the Storage Concept

Depending on the heat exchange mechanism between the heat transfer fluid and the storage medium, heat storage systems in CSP plants can be active or passive.

#### II.4.3.1. Active Storage Systems

The forced convection heat transfer in the storage material is the main feature of the active storage system. The storage medium circulates in a heat exchanger (which can be a solar receiver or a steam generator). [34]

Active systems are classified as direct or indirect.

The heat transfer fluid also acts as a storage fluid in the direct system, while the other fluid in the indirect system is used for heat storage. [34]

#### II.4.3.2. Passive Thermal Energy Storage

In a passive thermal storage system, the storage medium is non-circulating and consists primarily of a solid medium such as concrete or solid PCM. The thermal loading and unloading processes are based entirely on the circulation of the heat transfer fluid, which distributes the thermal energy to the solid via a heat exchanger integrated in the system [34].

Compared to other systems, this storage system offers the advantages of cheaper storage materials and a high heat transfer coefficient. However, the disadvantages of them are due to the additional cost of the heat exchanger and the instability that can occur during long periods of operation.

### II.4.4. Selection of Thermal Storage Medium

A variety of thermal mediums are used in CSP plants, including synthetic oil, molten salt, and steam. It is important to understand the properties of these fluids so that they can act as heat carriers. The properties of the liquids include, among other things, that they are non-toxic, non-flammable and non-explosive. In addition, it is imperative that the liquids have a high boiling point and a low freezing point to avoid the use of supplemental heating during the operation of the system. Ambient temperatures can decrease significantly over time due to transient weather conditions and convective/conductive heat transfer. The environment can also decrease the temperature of the medium significantly.

## II.5. Heat Transfer Modes

### II.5.1. Conduction:

Conduction is the transfer of heat through a solid material without the bulk movement of the material itself. It occurs due to the collision of adjacent atoms or molecules within the material. Heat is transferred from a region of higher temperature to a region of lower temperature through a series of molecular interactions. The rate of conduction depends on the thermal conductivity of the material, the temperature difference, and the cross-sectional area through which heat flows.

In the case of a wall, one dimensional heat transfer rate is described by Fourier's law of condition as:

$$q = -KA\frac{dy}{dx} \qquad \text{II.1}$$

**II.5.2. Convection:**

Convection is the transfer of heat through a fluid (liquid or gas) by the actual movement of the fluid itself. This movement can be natural (natural convection) or forced (forced convection).

The rate of energy transfer from the surface to the fluid can be quantified by Newton's law of convection as:

$$q = hA(T_S - T_\infty) \qquad \text{II.2}$$

II.5.2.1. Natural Convection

Heat transfer by natural convection occurs whenever a body is placed in a fluid at a higher or lower temperature than the body. Due to the difference in temperature, heat flows between the fluid and the body and causes a change in the density of fluid near the surface. [48]

The natural circulation of fluids is cauterized by the dimensionless Grashof number:

$$G_r = \frac{\beta g \Delta T \rho^2 L^3}{\mu^2} \qquad \text{II.3}$$

II.5.2.2. Forced Convection

In forced convection, the fluid moves over the surface at a high speed. This speed is often created by a pump (for liquids) or a fan or blower (for gases). [46]

The experimental data for forced convection are correlated through the use of three dimensionless numbers:

- The Reynolds number Re. $\text{Re} = \frac{\rho V D}{\mu}$ II. 4
- The Prandtl number Pr. $\text{Pr} = \frac{C_p \mu}{k}$ II. 5
- The Nusselt number Nu. $Nu = \frac{hD}{k}$ II. 6

The correlation of the experimental data gives the Nusselt number as a function of the other numbers:

$$Nu = f(Re, Pr, Gr) \qquad \text{II.7}$$

Once the Nusselt number is determined, the convective coefficient can be obtained from the definition of Nusselt number given in equation II.6.

II.5.2.3. Radiation:

Radiation is the transfer of heat in the form of electromagnetic waves and does not require a material medium to propagate. It can occur through a vacuum or through a transparent medium.

All objects emit thermal radiation as a function of their temperature. The rate of radiation heat transfer is proportional to the fourth power of the absolute temperature (Stefan-Boltzmann law) as

$$\dot{Q}_e = \varepsilon \sigma A T_b^4 \qquad \text{II.8}$$

With $\sigma = 5.64 \times 10^{-8}\ \mathrm{W/m^2.K^4}$

Surfaces can also absorb and reflect radiation based on their properties (emissivity and reflectivity).

## II.5.3. **Heat Flux**

The heat circulates under the influence of a temperature gradient from high to low temperature. The heat flux expression is given in terms of the change in the quantity of heat as a function of time and surface area of the isothermal surface is called the heat flux density:

$$\phi = \frac{1}{S}\frac{dQ}{dt} \qquad \text{II.9}$$

### II.5.4. Flow Regimes

Flow regimes are classifications of fluid flow based on the flow's behavior. The Roscommon classification is based on the Reynolds number.

The three main flow regimes are figure II-9:

**Laminar flow**: This is characterized by smooth, orderly flow with fluid layers moving parallel to each other. Laminar flow occurs at low Reynolds numbers Re<2300, where the viscous forces are dominant.

**Turbulent flow:** This is characterized by chaotic, irregular flow. Turbulent flow occurs at high Reynolds numbers Re>3000, where the inertial forces are dominant, the flow is **turbulent**

**Transitional flow**: This is a region between laminar and turbulent flow 2300<Re<3000

Where the flow behavior is unstable and can switch back and forth between the two regimes.

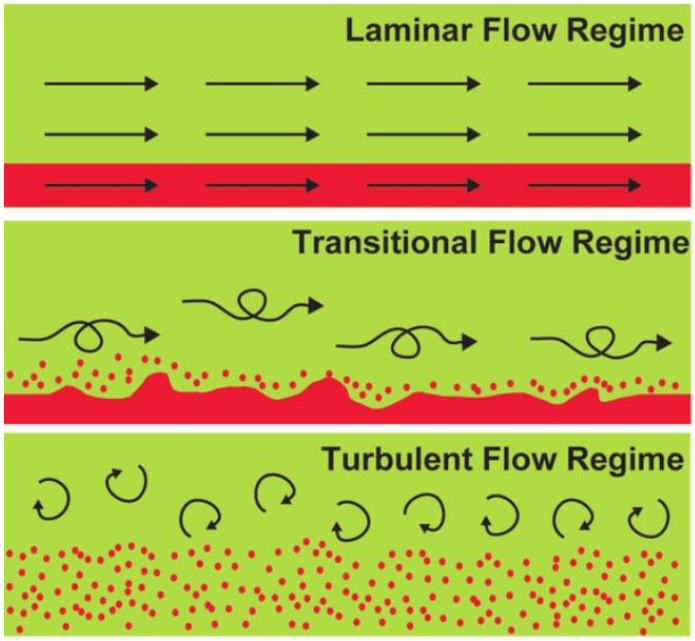


Figure II- 9: The flow regimes.

### II.5.5. Fluid Temperature

The fluid temperature changes and decreases, as heat is transferred through the tubes. Since the temperature of solid is less than the fluid temperature it absorbs heat from the fluid.

Fluid internal convection analysis with constant tube surface temperature is shown in figure II-10.

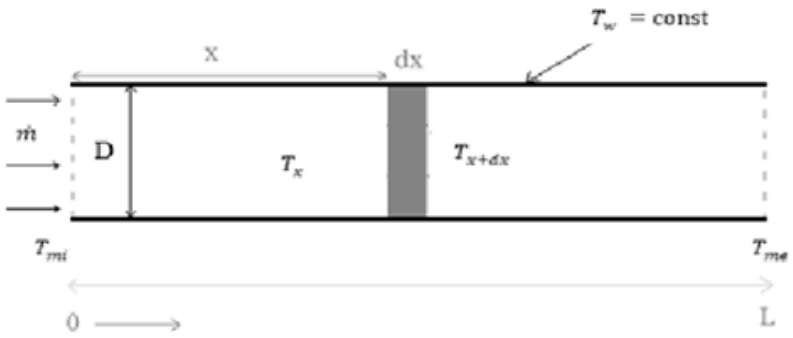


Figure II- 10: Internal convection in tube with constant surface temperature.

$$(\pi D dx)h(T_w - T_x) = \dot{m}C_p(T_{x+dx} - T_x) \qquad \text{II.10}$$

With, $T_{x+dx}$=$T_x + \mathrm{d}T_x$ ; $\dot{m} = \rho A v$ and A= $\pi D dx$.

$$h\pi D dx(T_w - T_x) = \dot{m}C_p(T_x + \mathrm{d}T_x - T_x)$$

$$\int_{x=0}^{x} \frac{\pi D h}{\dot{m}C_p}\mathrm{dx} = \int_{T_{mi}}^{T_x} \frac{1}{(T_w - T_x)}\mathrm{d}T_x$$

Becomes: $$-\frac{\pi D h x}{\dot{m}C_p} = +ln(T_w - T_x) - ln(T_w - T_{mi})$$

$$\ln\left(\frac{T_x - T_w}{T_{mi} - T_w}\right) = -\frac{\pi D h x}{\dot{m}C_p}$$

The temperature of the liquid $T_x$ in the tube is calculated based on the temperature of the inlet liquid temperature.

$$T_x = e^{\frac{-\pi D h x}{\dot{m}C_p}}(T_{mi} - Tw) + Tw \qquad \text{II. 11}$$

The equation II.11 represents how the temperature at a certain point within the fiuid changes due to the combined effects of heat conduction and convection into or out of the fluid.

### II.5.6. Energy Balance Equation of PTC

In this section, a theoretical study is presented. The thermal performance of PTC is characterised by an energy balance based on the laws of thermodynamics. The theoretical model considers the thermo-physical, optical and geometrical parameters of the PTC.

The thermal balance of the system is written for a time interval in the following form:

$$Qu = A_c[(\tau\alpha)_c G^* - \frac{A_r}{A_c} U_L(T_p - T_a)] \qquad \text{II.12}$$

Where, $Qu$ is the useful energy rate; $A_c and A_r$are the concentrator area and receiver area, respectively; $(\tau\alpha)_c$ is the absorptance-transmittance product; $G^*$ is the incident global solar irradiation; $T_a$ and $T_p$ are ambient and absorber plate temperature, respectively and $U_L$ is the overall heat loss coefficient.

II.5.6.1. Concentration Ratio

A solar concentrator is a device that concentrates the solar radiation falling on a larger surface (aperture area, Ac) onto a smaller surface (receiver area, Ar). The concentration ratio can be calculating as follows:

$$C = \frac{A_r}{A_c} \qquad \text{II.13}$$

II.5.6.2. Overall heat loss coefficient

II.5.6.2.1 Top heat loss coefficient

The heat transfer coefficient by convection from the absorber plate to the cover $h_{1c}$ can be written as follows

$$h_{1c} = N_u \frac{K_f}{L_f} \quad \text{II.14}$$

Where $K_f$ and $L_f$ are the fluid thermal conductivity and the spacing between absorber plate and transparent cove, respectively. However, if the gap between absorber plate and cover is evacuated, the heat transfer coefficient by convection is negligible ($h_{1c} \approx 0$).

The heat transfer coefficient by radiation from the absorber plate to the cover $h_{1r}$is given as follows

$$h_{1r} = \frac{\sigma(T_p{}^2 + T_c{}^2)(T_p + T_c)}{\frac{1-\varepsilon_p}{\varepsilon_p} + \frac{(1-\varepsilon_c)A_r}{\varepsilon_c A_g} + 1} \qquad \text{II.15}$$

Here $A_g$ is the glass cover area; $T_c$ is the cover temperature; $\varepsilon_c$ and $\varepsilon_p$ are cover and absorber plate emissivity, respectively and $\sigma = 5.67\ 10^{-8}$ is Stefan's constant.

The heat transfer coefficient by convection from the cover to the ambient $h_{2c}$is calculated by Watmuff et al. (1977) correlation.

$$h_{2c} = 2{,}8 + 3v_{wind} \qquad \text{II.16}$$

Here $v_{wind}$is wind speed over the collector transparent cover.

The heat transfer coefficient by radiation from the cover to the ambient $h_{2r}$is given as a function of the sky temperature $T_{sky}$ and the outside cover face temperature $T_c$.

$$h_{2r} = \frac{\sigma \varepsilon_c \left(T_c^4 - T_{sky}^4\right)}{T_c - T_a} \qquad \text{II.17}$$

The top heat loss coefficient $U_t$ is expressed as:

$$U_t = \left(\frac{1}{h_{1r}} + \frac{1}{h_{2c}+h_{2r}}\right)^{-1} \qquad \text{II.18}$$

II.5.6.2.2 Back heat loss coefficient

Back heat loss coefficient can be calculated same as top heat loss coefficient.

$$U_b = \left(\frac{1}{h_{3r}} + \frac{1}{h_{4c}+h_{4r}}\right)^{-1} \qquad \text{II.19}$$

Assuming that all heat losses are to an ambient temperature, the overall heat loss coefficient$U_L$is the summation of the top and back heat loss coefficients.

$$U_L = U_t + U_b = \left(\frac{1}{h_{1r}} + \frac{1}{h_{2c}+h_{2r}}\right)^{-1} + \left(\frac{1}{h_{3r}} + \frac{1}{h_{4c}+h_{4r}}\right)^{-1} \qquad \text{II.20}$$

II.5.6.3. Outlet Fluid Temperature

The useful energy gained by an absorber sheet of width $W$, length $L_{tb}$ and thickness $e_p$ is transferred to the pipe of exterior/interior diameters $Do/di$, thickness $e_t$ and thermal conductivity $\lambda_t$. A working fluid of specific heat $c_f$ and mass flow rate $\dot{m}_f$ passes through this tube. The main collector factors can be determined as follows:

*Sheet efficiency factor F*

$$F = \frac{\tanh\left[m\left(\frac{W-Do}{2}\right)\right]}{m\left(\frac{W-Do}{2}\right)} \qquad \text{II.21}$$

*Collector efficiency factor$F'$*

$$F' = \frac{1}{W L_{tb} U_L \left[\frac{1}{[(W-Do)F+Do]U_L} + \frac{e_{tb}}{\pi A_{mw} \lambda_t} + \frac{1}{\pi di h_f}\right]} \qquad \text{II.22}$$

*Heat removal factor$F_R$*

$$F_R = \frac{\dot{m}_f C_f}{U_L}\left(1 - exp\left(-\frac{nF' W L_{tb} U_L}{\dot{m}_f c_f}\right)\right) \qquad \text{II.23}$$

The above equations used to rewrite the maximum useful energy rate as follows:

$$Qu = A_c F_R[(\tau\alpha)_c G^* - C * U_L(T_{fi} - T_a)] \qquad \text{II.24}$$

The mean absorber plate $T_p$ and mean outlet fluid $T_{fo}$ temperature can be calculated as follows:

$$T_p = T_{fi} + \frac{Qu}{A_c F_R U_L}(1 - F_R) \qquad \text{II.25}$$

$$T_{fo} = T_{fi} + \frac{Qu}{A_c F_R U_L}\left(1 - \frac{F_R}{F'}\right) \qquad \text{II.26}$$

### II.5.7. Defining Heat Transfer Problem

Formulating a heat transfer problem involves defining the problem statement, specifying the governing equations, boundary conditions, and material properties.

II.5.7.1. Define the Problem Statement:

Calculating the temperature distribution within a solid object subjected to a specific heat source and understanding how heat is transferred through a system.

II.5.7.2. Specify the Governing Equations:

In heat transfer problems, the fundamental equation is the heat conduction equation, which is a partial differential equation (PDE). It describes how temperature changes with respect to time and space.

II.5.7.3. Define Boundary Conditions:

Boundary conditions are essential for solving the heat transfer problem. They specify the temperature or heat flux at the boundaries of the system.

II.5.7.4. Specify Material Properties:

The material properties of the solid (or fluid) through which heat is transferred are crucial. This includes the thermal conductivity (k), specific heat capacity (Cp), and density (ρ) of the material. These properties are often temperature-dependent and may require reference sources for accurate values.

II.5.7.5. Consider Heat Generation or Sources:

If there are internal heat sources or sinks within the system (Q in the heat conduction equation), it's necessary to define these sources mathematically. This could include electrical heating, chemical reactions, or other energy inputs.

II.5.7.6. Choosing Appropriate Coordinates and Dimensions:

Determine whether the problem is one-dimensional (1D), two-dimensional (2D), or three-dimensional (3D). The choice of dimensions affects the complexity of the problem.

II.5.7.7. Specify Time Dependency:

Determine whether the problem is steady-state (temperature does not change with time) or transient (temperature changes with time). Transient problems involve time-dependent variations and require additional equations.

II.5.7.8. Using Appropriate Modeling Assumptions:

Simplify the problem as needed by making reasonable assumptions. For instance, assuming steady-state conditions or neglecting certain terms in the heat conduction equation can simplify the problem.

II.5.7.9. Solve the Problem Numerically:

Depending on the complexity of the problem, it's important to use numerical methods (e.g., finite difference, finite element, or finite volume methods) to solve the governing equations. By following these steps and referencing appropriate sources, it will be easy to formulate and solve a heat transfer problem accurately and reliably.

## II.6. Finite Difference Method:

The finite difference method (FDM) is a numerical technique used for approximating solutions to differential equations, especially partial differential equations (PDEs). It discretizes the spatial and sometimes temporal domain into a grid of points and approximates derivatives using finite differences. This method is widely used in various fields of science and engineering, such as heat transfer, fluid dynamics, electromagnetism, and finance.

### II.6.1. Discretization of the Domain:

The first step in the FDM is to discretize the spatial and temporal domain of the problem. This involves dividing the domain into a grid of discrete points. In one dimension (1D), this means dividing the domain into intervals, while in two dimensions (2D) or three dimensions (3D), it involves creating a grid or mesh.

### II.6.2. Discretization of the Differential Equations:

The next step is to approximate the derivatives in the differential equations using finite difference formulas. These formulas estimate the derivatives at each grid point by considering neighboring grid points. The choice of finite difference formula depends on the type of derivative (first-order, second-order, etc.) and the accuracy required for the problem. Common finite difference formulas include central differences, forward differences, and backward differences.

### II.6.3. Formulation of Discrete Equations:

Using the finite difference approximations, it'll be easy to transform the original differential equations into a set of discrete equations. These equations are typically algebraic equations that relate the values of the dependent variable at different grid points.

### II.6.4. Boundary and Initial Conditions:

Boundary conditions (for spatial domains) and initial conditions (for time-dependent problems) are imposed at the corresponding grid points. These conditions provide information about the behavior of the system at the boundaries or at the initial time.

### II.6.5. Solution of the Discrete Equations:

The resulting system of discrete equations can be solved using numerical techniques such as iterative methods (e.g., Gauss-Seidel or Jacobi) or direct solvers (e.g., LU decomposition), in this case we choose Gauss-Seidel method.

The solution provides the values of the dependent variable at all grid points.

### II.6.6. Post-processing and Analysis:

After obtaining the numerical solution, post-process the data to extract relevant information or perform further analysis. This may include visualizing results, computing derived quantities, or evaluating the accuracy of the solution.

To conclude, the mathematical model of two-dimensional heat conduction in the unsteady state without an internal heat source is expressed as follows:

$$\frac{\partial^2 T}{\partial^2 x} + \frac{\partial^2 T}{\partial^2 y} = \frac{1}{\alpha}\frac{\partial T}{\partial t} \qquad \text{II.27}$$

Applying the first heat conduction equation in (II.13) to node (i, j) at time t, the equation can be rewritten as follows:

$$\left(\frac{\partial^2 T}{\partial^2 x}+\frac{\partial^2 T}{\partial^2 y}\right)_{i,j}^{t}=\frac{1}{\alpha}\left(\frac{\partial T}{\partial t}\right)_{i,j}^{t} \qquad \text{II.28}$$

The partial differential of both sides of (II.29) can be approximated by a quotient of difference. The temperature element to the right of the equal sign can be approximated by the time difference quotient of first order.

$$\left(\frac{\partial T}{\partial t}\right)_{i,j}^{t}=\frac{T_{i,j}^{t+1}-T_{i,j}^{t}}{\Delta t} \qquad \text{II.29}$$

The partial differential of the second order to the left of the equal sign can be approximated by an explicit or implicit method.

## II.7. Types of Finite Difference Methods:

### II.7.1. Implicit Method:

Here, the solution involves unknown values at the current time step (t) of the system and the future state (t+1) and is solved using a system of equations. Implicit methods are often more stable but require solving larger systems of equations.

Thus, we can write the following for the problem in question.

$$\left(\frac{\partial^2 T}{\partial^2 x}+\frac{\partial^2 T}{\partial^2 y}\right)_{i,j}^{t}=\frac{T_{i+1,j}^{t+1}-2T_{i,j}^{t+1}+T_{Ti-1,j}^{t+1}}{\Delta x^2}+\frac{T_{i,j+1}^{t+1}-2T_{i,j}^{t+1}+T_{Tij-1}^{t+1}}{\Delta y^2} \qquad \text{II.30}$$

Substituting (II.30) and (II.31) into (II.29) and taking $\Delta x = \Delta y$, we can write the total equation as follows:

$$\frac{T_{i,j}^{t+1}-T_{i,j}^{t}}{\Delta t}=\alpha\frac{-4T_{i,j}^{t+1}+T_{i+1,j}^{t+1}+T_{Ti-1,j}^{t+1}+T_{i,j+1}^{t+1}+T_{Ti,j-1}^{t+1}}{\Delta x^2} \qquad \text{II.31}$$

### II.7.2. Explicit Method:

In this approach, the solution at a given time step is computed explicitly in terms of known values at the previous time step. It is straightforward but may have stability limitations, especially for stiff problems.

Considering (II.29), the explicit finite difference method can be employed as follows:

$$\left(\frac{\partial^2 T}{\partial^2 x}+\frac{\partial^2 T}{\partial^2 y}\right)_{i,j}^{t}=\frac{T_{i+1,j}^{t}-2T_{i,j}^{t}+T_{Ti-1,j}^{t}}{\Delta x^2}+\frac{T_{i,j+1}^{t}-2T_{i,j}^{t}+T_{Ti,j-1}^{t}}{\Delta y^2} \qquad \text{II.32}$$

Substituting (II.30) and (II.33) into (II.29) and taking $\Delta x = \Delta y$ , we can write the total equation as follows:

$$\frac{T_{i,j}^{t+1}-T_{i,j}^{t}}{\Delta t}=\alpha\frac{T_{i,j+1}^{t}-2T_{i,j}^{t}+T_{Ti,j-1}^{t}+T_{i+1,j}^{t}-2T_{i,j}^{t}+T_{Ti-1,j}^{t}}{\Delta x^2} \qquad \text{II.33}$$

## II.8. Nodal Energy Balance Equations

The nodal energy balance equation is a fundamental equation in heat transfer that expresses the conservation of energy at a node. It states that the net rate of heat transfer into a node must equal the rate of change of energy stored in the node.

The general nodal energy balance equation is: ∑Q_in - ∑Q_out = ΔE_node where:

-∑Q_in: is the sum of all the heat transfer rates into the node

-∑Q_out: is the sum of all the heat transfer rates out of the node

-ΔE_node: is the change in energy stored in the node in situations where there is no internal energy generation, the nodal energy balance equation simplifies to:

$$\sum Q_{in} = \sum Q_{out} \qquad \text{II.34}$$

This means that the net rate of heat transfer into a node must equal the net rate of heat transfer out of the node.

The nodal energy balance equation can be applied to any node in a heat transfer system. The node can be a single point, a surface, or a volume. The equation can also be applied to steady-state or transient systems.

With the help of **Dr. Yilma.T** article [35] nodal energy balance equations relevant to several common configurations for situations where there is no internal energy generation are presented as follows:

### II.8.1. Internal Node:

Thermal balance of an internal node is presented in figure II-12.

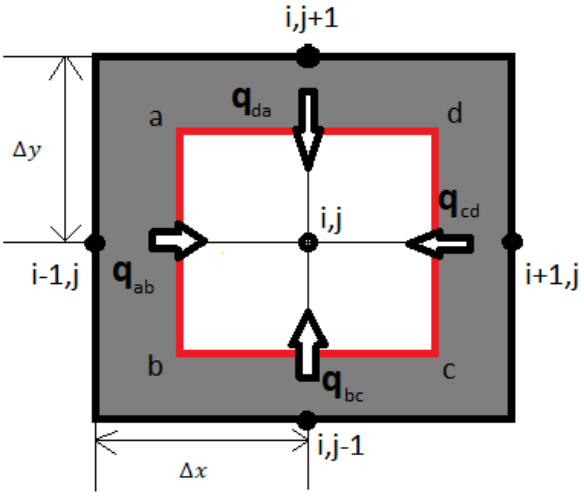


Figure II- 12: Thermal balance of an internal node.

Assuming no heat generation inside the system equation II.34 becomes:

$$q_{ab} + q_{bc} + q_{cd} + q_{da} = mcp\frac{dT}{dt}$$

$$-K\Delta y\frac{T_{i,j}^{t} - T_{i,1,j}^{t}}{\Delta x} - K\Delta y\frac{T_{i,j}^{t} - T_{i+1,j}^{t}}{\Delta x} - K\Delta x\frac{T_{i,j}^{t} - T_{i,j-1}^{t}}{\Delta y} - K\Delta x\frac{T_{i,j}^{t} - T_{i,j+1}^{t}}{\Delta y} = \rho c_p\frac{T_{i,j}^{t+\Delta t} - T_{i,j}^{t}}{\Delta t}$$

With : $m = \rho v = \rho.\Delta x \cdot \Delta y \cdot \Delta z$

Therefore, the temperature at the internal node is calculated according to equation:

$$T_{i,j}^{t+\Delta t} = (1 + 4F_0)T_{i,j}^{t} - F_0\left(+T_{i-1,j}^{t} + T_{i+1,j}^{t} + T_{i,j-1}^{t} + T_{i,j+1}^{t}\right) \qquad \text{II.35}$$

For stability, the coefficient on $T_{i,j}^{t}$ in II.35 must be non-negative so we can write:

$1 - 4F_0 \geq 0$

### II.8.2. External Node on a Flat Surface

II.8.2.1. With Convection Condition:

This node represents a point, a location on a surface or a boundary with a fluid is shown in figure II-13.

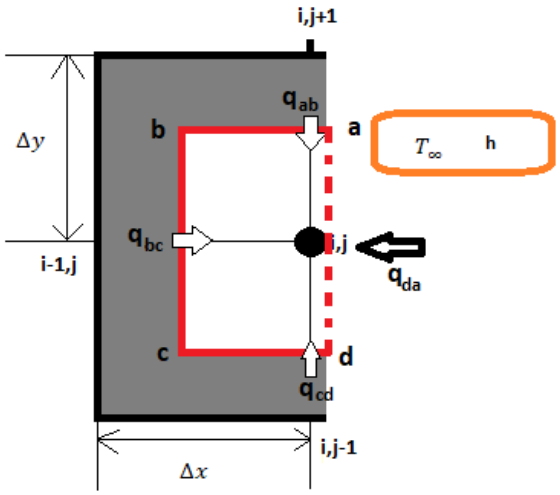


Figure II- 13: Node on a flat surface with convection.

With no heat generation inside the system, the energy balance equation for node at plane surface in contact with fluid can be given as:

$$q_{ab} + q_{bc} + q_{cd} + q_{da} = mcp\frac{dT}{dt}$$

$$-K\Delta y\frac{T_{i,j}^{t} - T_{i-1,j}^{t}}{\Delta x} - K\frac{\Delta x}{2}\frac{T_{i,j}^{t} - T_{i,j-1}^{t}}{\Delta y} - K\frac{\Delta x}{2}\frac{T_{i,j}^{t} - T_{i,j+1}^{t}}{\Delta y} - h\Delta x\left(T_{i,j}^{t} - T_\infty\right) = \rho\frac{\Delta x^2}{2}c_p\frac{T_{i,j}^{t+\Delta t} - T_{i,j}^{t}}{\Delta t}$$

Hence the temperature at the boundary node in contact with a fluid is calculated according to the equation.

$$\left(1 - 2F_0(B_i + 2)\right)T_{i,j}^{t} + F_0\left(T_{i,j-1}^{t} + 2T_{i-1,j}^{t} + T_{i+1,j}^{t} + 2B_iF_0T_\infty^{t}\right) = T_{i,j}^{t+\Delta t} \qquad \text{II.36}$$

For stability, the coefficient on $T_{i,j}^{t}$ in (II.36) must be non-negative, so we can write:

$$1 - 2F_0(B_i + 2) > 0$$

II.8.2.2. With Adiabatic Condition:

This node represents a point or location on a surface that has an adiabatic boundary as shown in figure II-14.

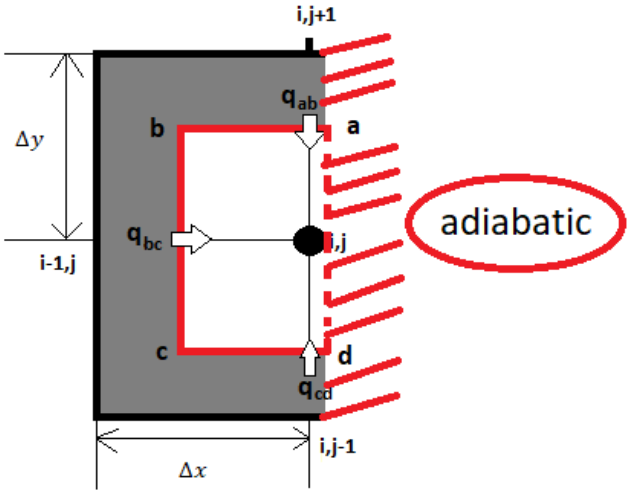


Figure II- 14: Node on a flat surface with adiabatic condition.

With no heat generation inside the system, the energy balance equation for node at plane surface with adiabatic boundary condition can be given as:

$$q_{ab} + q_{bc} + q_{cd} + q_{da} = mcp\frac{dT}{dt}$$

$$-K\Delta y\frac{T_{i-1,j}^{t} - T_{i,j}^{t}}{\Delta x} - K\frac{\Delta x}{2}\frac{T_{i,j}^{t} - T_{i,j+1}^{t}}{\Delta y} - K\frac{\Delta x}{2}\frac{T_{i,j}^{t} - T_{i,j-1}^{t}}{\Delta y} = \rho\frac{\Delta x^2}{2}c_p\frac{T_{i,j}^{t+\Delta t} - T_{i,j}^{t}}{\Delta t}$$

The temperature at the adiabatic boundary node is calculated according to the equation:

$$(1 - 4F_0)T_{i,j}^{t} + F_0\left(T_{i,j-1}^{t} + T_{i-1,j}^{t} + T_{i+1,j}^{t}\right) = T_{i,j}^{t+\Delta t} \qquad \text{II.37}$$

### II.8.3. Exterior Corner Node

II.8.3.1. Convection-Adiabatic Condition:

This node represents corner with convection-adiabatic condition as shown in figure II-15.

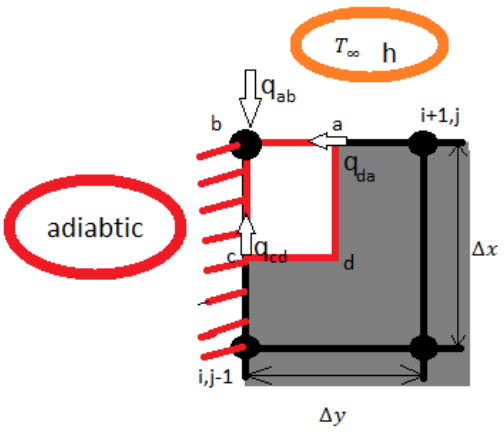


Figure II- 15: Node at an external corner with convection-adiabatic condition.

With no heat generation inside the system, the energy balance equation for node at exterior corner with convection-adiabatic condition can be given as:

$$q_{ab} + q_{bc} + q_{cd} + q_{da} = mcp\frac{dT}{dt}$$

$$-K\frac{\Delta y}{2}\frac{T_{i,j}^t - T_{i+1,j}^t}{\Delta x} - K\frac{\Delta x}{2}\frac{T_{i,j}^t - T_{i,j-1}^t}{\Delta y} - h\Delta x\left(T_{i,j}^t - T_\infty\right) = \rho\frac{\Delta x^2}{2}c_p\frac{T_{i,j}^{t+\Delta t} - T_{i,j}^t}{\Delta t}$$

The temperature in this case is calculated according to the equation:

$$\left(1 - 2F_0(B_i + 2)\right)T_{i,j}^t + 2F_0\left(T_{i+1,j}^t + T_{i,j-1}^t + 2B_iF_0T_\infty^t\right) = T_{i,j}^{t+\Delta t} \qquad \text{II.38}$$

For stability, the coefficient on $T_{i,j}^t$ in II.39 must be non-negative so, we can

Write:

$$1 - 2F_0(2 + B_i) > 0$$

II.8.3.2. Adiabatic-Symmetric Condition:

This node represents corner with adiabatic - symmetric condition as shown in figure II-16.

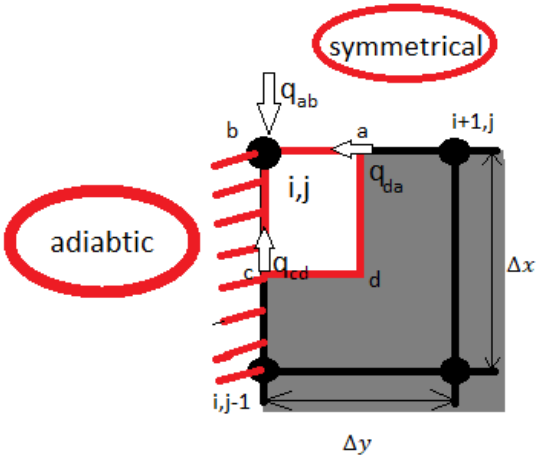


Figure II- 16: Node at an outer corner with adiabatic- symmetric condition.

With no heat generation inside the system, the energy balance equation for node at exterior corner with adiabatic- symmetric condition can be given as:

$$q_{ab} + q_{bc} + q_{cd} + q_{da} = mcp\frac{dT}{dt}$$

$$-K\frac{\Delta y}{2}\frac{T_{i,j}^{t} - T_{i+1,j}^{t}}{\Delta x} - K\frac{\Delta x}{2}\frac{T_{i,j}^{t} - T_{i,j-1}^{t}}{\Delta y} = \rho\frac{\Delta x^2}{2}c_p\frac{T_{i,j}^{t+\Delta t} - T_{i,j}^{t}}{\Delta t}$$

The temperature in this case is calculated according to the equation:

$$(1 - 4F_0)T_{i,j}^{t+\Delta t} + 2F_0\left(T_{i+1,j}^{t} + T_{i,j-1}^{t}\right) = T_{i,j}^{t+\Delta t} \qquad \text{II.39}$$

## II.9. Thermodynamic Equations:

### II.9.1. Rankine Cycle

The Rankine cycle, figure II-17, is an idealized thermodynamic cycle of a constant pressure heat engine that converts part of heat into mechanical work. In this cycle, the heat is supplied externally to a closed loop, which usually uses water (in a liquid and vapor phase) as the working fluid. In an ideal Rankine cycle, the system executing the cycle undergoes a series of four processes: two isentropic (reversible adiabatic) processes alternated with two isobaric processes:

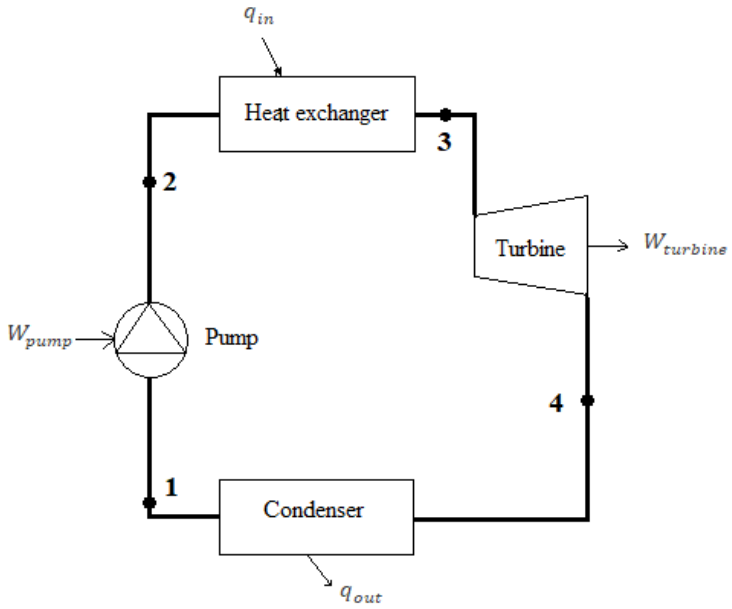


Figure II- 17: Schematic of the Rankine cycle.

II.9.1.1. Isentropic Compression (Processes 1-2):

In this initial stage, water is pumped from a low-pressure state (state 1) to a higher-pressure state (state 2). This process is typically considered isentropic, meaning it is adiabatic and reversible.

The work required for the compressor is given by $W_P = h_1 - h_2$ II.40

II.9.1.2. Isobaric Heat Addition (Processes 2-3):

In this stage, the high-pressure water is heated at a constant pressure in a heat exchanger.

The heat added during this process is given by:

$$Q_{add} = h_3 - h_2 \qquad \text{II.41}$$

II.9.1.3. Isentropic Expansion (Processes 3-4):

The high-pressure, high-temperature steam is expanded through a turbine, generating mechanical work.

The work output from the turbine is given by:

$$WT = h3 - h4 \qquad \text{II.42}$$

II.9.1.4. Isobaric Heat Rejection (Processes 4-1):

In this stage, the low-pressure steam is condensed back into a liquid in a condenser, releasing heat.

The heat rejected during this process is given by:

$$\mathbf{Q_{re} = h_4 - h_1} \qquad \text{II.43}$$

II.9.1.5. Efficiency of the Rankine Cycle may be written as:

$$\eta = \frac{W_{nut}}{Q_{add}} \qquad \text{II.44}$$

With:

$W_{nut} = W_p + W_T$

## II.10. Heat Exchanger

Heat exchangers, figure II-18, are devices that transfer heat from one fluid to another without mixing them. They are used in a wide range of applications power generation, and industrial processes.Heat exchangers are designed to maximize the rate of heat transfer between the two fluids. This is done by using a variety of techniques, such as increasing the surface area of the heat exchanger, increasing the flow rate of the fluids, and using materials with high thermal conductivity. They are an essential part of many different industries and applications and used to improve energy efficiency, reduce emissions, and provide a reliable source of heating and cooling. [36]

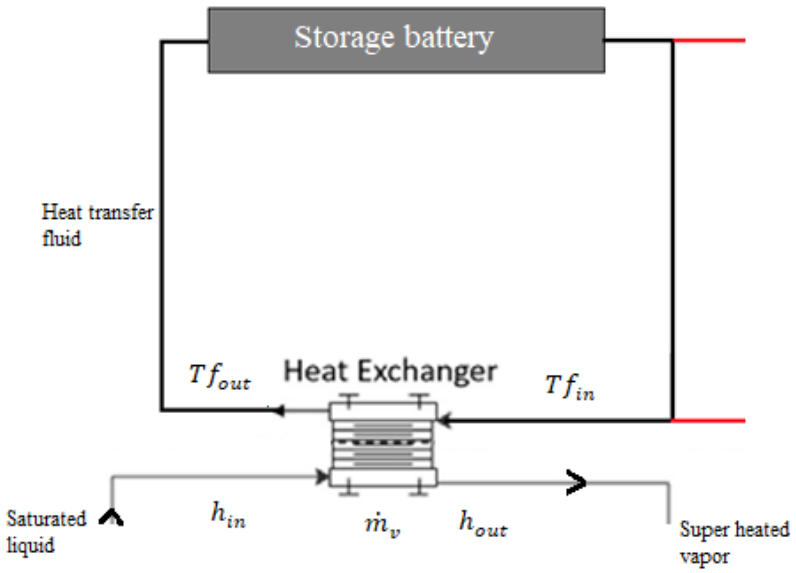


Figure II- 18: Diagram of heat exchanger combined with storage battery.

### II.10.1. Heat Exchanger Energy Balance

Heat exchanger energy balance is the principle that the net heat transfer to a heat exchanger must be equal to the net heat transfer from the heat exchanger. Figure II- 19

In the case of a heat exchanger, the system is the fluids inside the exchanger. The net heat transfer into the system is the sum of the heat transfer rates from the hot and cold fluids. The change in internal energy of the system is the sum of the changes in internal energy of the hot and cold fluids. The net work done by the system is zero, since the fluids are assumed to be stationary.

$$Q_1 + Q_2 + Q_{1,l} + Q_{2,l} + Q_{3,l} = 0 \qquad \text{II.45}$$

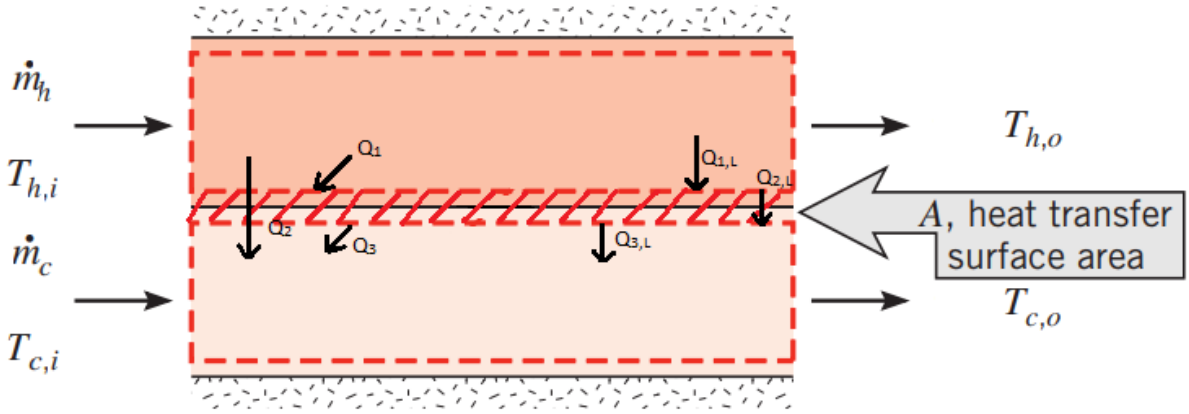


Figure II- 20: Overall energy balances for the hot and cold fluids of a two-fluid heat exchanger. [36]

The energy balance on a heat exchanger can be used to determine the heat transfer rate, the outlet temperatures of the fluids, or the flow rates of the fluids. It can also be used to design heat exchangers and to evaluate their performance.

$$\dot{Q}_{Hf} = \dot{Q}_V + \dot{Q}_F \qquad \text{II.46}$$

Efficiency of the heat exchanger may be written as:

$$\eta_{He} = \frac{\dot{Q}_V}{\dot{Q}_{Hf}} \qquad \text{II.47}$$

Using the equation II.46 and equation II.47 was found**:**

$$\dot{m}_v(h_{out} - h_{in}) = -\eta_{He}\dot{m}_f c_p(Tf_{out} - Tf_{in}) \qquad \text{II.48}$$

$h_{in}$ is the inlet enthalpy of heat exchanger.

$h_{out}$ is the outlet enthalpy of heat exchanger.

$T_{f\,out}$ is the outlet temperature of heat transfer in heat exchanger.

$T_{f\,in}$ is the inlet temperature of heat transfer fluid in heat exchanger.

When the temperature of the heat transfer fluid coming from the battery or from the collector becomes so high that the temperature of the water after the heat exchanger reaches more than 100°C, steam is generated.

### II.10.2. Efficiency of Storage Battery:

The efficiency value is expressed on the extent of the battery's carrying capacity in saving and storing thermal energy and is calculated:

$$\eta = \frac{Q_{RE}}{Q_T} \qquad \textbf{II.49}$$

$\boldsymbol{Q_{RE}}$ : Thermal energy output by the battery**.**

$\boldsymbol{Q_T}$ : thermal **energy** received by the battery.

# Chapter III

# Calculation Algorithm and Studied Case

## III.1.Introduction

Thermal energy storage devices TES have aroused great interest among researchers due to their applications in eliminating environmental problems and improving energy efficiency. TES systems store thermal energy in hot or cold materials for later use.

However, it should be noted here that the development of numerical models and simulation analyzes has largely contributed to a better understanding of the operational performance of TES systems.

This chapter explains the algorithms of the program.

## III.2.Heat Storage Algorithm:

The developed program which is the continuity of the work of Rahal.A and Khalifa med. A [17] consistent of the following parts.

### III.2.1.Data Entry

The length , width , number of rows, number of columns, initial temperature of the solid, initial temperature of the fluid, density, specific heat of solid and fluid density, specific heat of solid and fluid, number of time iterations, thermal conductivity, fluid velocity, diameter, dynamic viscosity.

### III.2.2.Calculation of Constants

The step of space: $dx = dy = \frac{L}{NX-1} = \frac{W}{NY-1}$

The thermal diffusivity α by the equation: $\alpha = \frac{K}{\rho C_P}$

The Fourier number: $F_0 = \frac{\alpha \Delta t}{\Delta x^2}$

Taking into account the stabilities criterion: $1 - 2F_0(2 + B_i) > 0$; so from there, the time space is determined as follows: $dt = \frac{dx^2}{3(2+Bi)*\alpha}$

The mass flow rate: $\dot{m} = \rho V A$

### III.2.3.The Initial Temperature of the Solid

All nodes of solid are equal to Ti at t=0s

### III.2.4.Fluid Temperature

The temperature changes from one node to another and is calculated using equation $II.11$

For the calculation and use equation $II.11$ in order to calculate it between tow nodes, the equation $II.11$must be modified. The temperature between two adjacent nodes is considered constant because between one node and the other very closed and their temperature deffence is slite.

$$Tf_{i+1} = e^{\frac{-\pi Dhx}{\dot{m}C_p}}(Tf_i - Tw) + Tw \qquad \text{III.1}$$

When $Tw = \frac{T_{i+}T_{i+1}}{2}$

$Tw$ : the mean temperature of tow adjacent nodes (considered as constat).

III.2.4.1. The Locale Reynolds number, Prandt number and Nusselt number are calculated as:

$$\text{Re} = \frac{\rho VD}{\mu}$$

$$\text{Pr} = \frac{C_p \mu}{k}$$

$$Nu = \frac{hD}{k}$$

If Re<2300 so Nu=4.36
If it differs from this condition so

Nu=0.023*(Re^0.8)*(Pr^(1/3));

III.2.4.2. The locale convection coefficient and Biot number are calculated as:

$$h = \frac{Nu\ D}{D}$$

$$Bi = \frac{hdx}{k}$$

### III.2.5. Calculation of Number of Iterations of the Storage

In this case only 8 hours and 20 minutes of charging are considered.
8 h and 20 minutes = 30000 s
P= 30000/dt represent the number of iterations of storage.

### III.2.6. Solid Temperature Calculation

- The temperature of the adiabatic convection corners nodes are calculated for left and right corner using equation II.38
- The temperature of the nodes situated in the surface with convection are calculated using equation II.36:

- The temperature of internal nodes are calculated using equation II.35
- The temperature of adiabatic-symmetric corners nodes of the left and right corner are calculated using equation II.39
- The temperature of nodes situated in adiabatic surfaces is are calculated using equation II.37

### III.2.7. Heat Release Algorithm

Initial temperature of the battery at release is the same as it temperature at 8h and 20min (the end of charging time). Now the heat exchanger, replace solar collectors and the output temperature of heat exchanger is the inlet temperature of the battery this temperature is calculated using equation II.31.

After simplifying, the expression of the temperature output from the heat exchanger in the following form:

$$Tf_{out} = Tf_{in} + \frac{\dot{m}_v(h_{out} - h_{in})}{-0.95\dot{m}_f c_p} \qquad \text{III-2}$$

Locale Reynolds number, Prandut number, Nusselt number and Biot number are calculated.

The locale convection coefficient and Biot number are calculated using equations:

$$h = \frac{Nu\ D}{D}$$

$$Bi = \frac{hdx}{k}$$

### III.2.8. Calculation of Number of Iterations of Discharge

8h and 20min of charging gives 15hours and 40min of discharging .

The temperatures of the liquid for each node are calculated as described in section III.2.4.

Locale Reynolds number Prandut number, Nusselt and Biot number are calculated.

The temperature of the solid and heat energy released in the discharge is calculated similary as charging process.

## III.3.Description of the Studied Configuration

The typical layout of a parabolic-through concentrating thermal solar power plant is illustrated in figure III- 1. It consists of a parabolic-through collectors, thermal storage battery and rankin cycle (heat exchanger, pump, condenser and turbine).

First, solar collectors with a parabolic trough receive the sun's rays so that they are reflected on the collector tube containing a heat transfer fluid. The liquid (liquid-sodium) absorbs heat and moves to the thermal storage battery where the heat is stored to be explore during night periods or periods of cloudy weather.

Then, heat transfer fluid passes through the heat exchanger and gives its thermal energy to the saturated water coming from the pump. So that the saturated water is converted into superheated steam.

Steam is used to run the steam turbine that generates mechanical energy which is converted into electrical energy through the electrical generator.

The steam coming out of the turbine passes through the condenser to be condensed and converted into saturated water. Saturated water passes through the pump, its pressure rise and move to the heat exchanger again and this cycle is called the Rankine cycle .

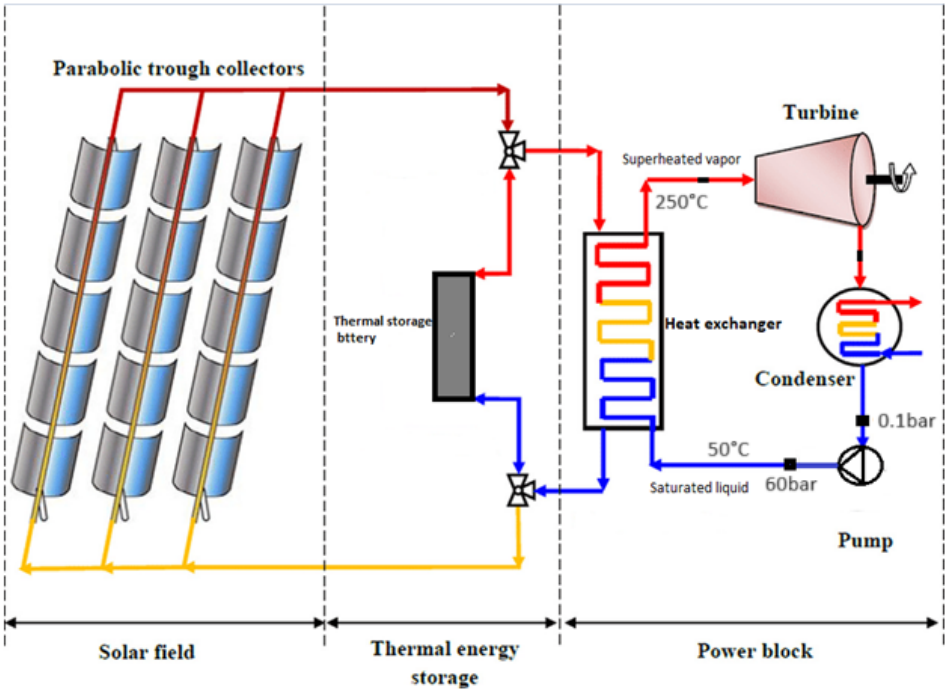


Figure III 1: Layout of a parabolic-through concentrating thermal solar power plant with thermal energy storage.

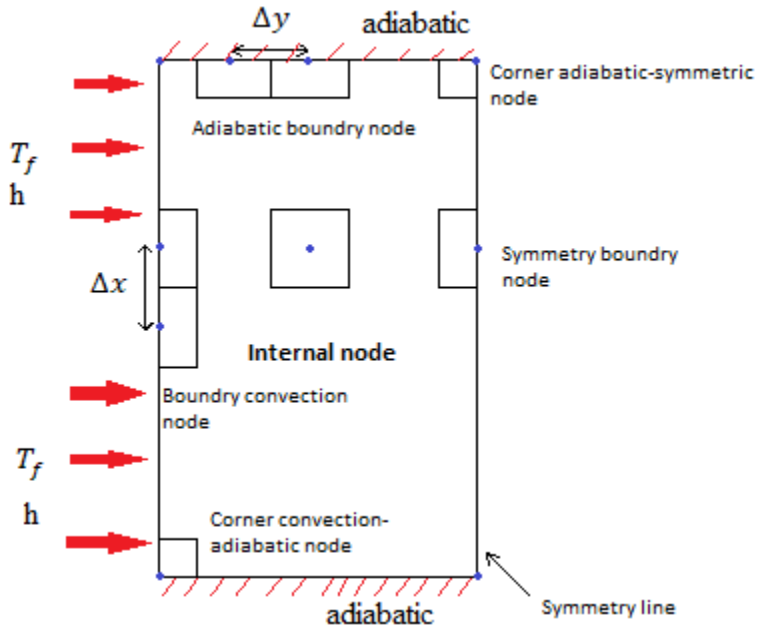


Figure III 2: Boundaries conditions.

- **The Initial Conditions:**
  1. The initial temperature distribution in the storage volume (solid) is 98 °C.
  2. The inlet temperature of the heat transfer fluid is time-variable during the day, as given it from a simulation of the parabolic trough collector

The limited conditions applied are shown in figure III-2:

- For symmetric boundary nodes, the symmetry condition.
- As for adiabatic boundary nodes adiabatic conditions

The temperature of the heat transfer fluid will vary over time and space according to equation $II.11$.

The thermo physical properties of the solid are illustrated on the following table:

Table III-1: Properties of the storage materials Concrete.

| Material | Density [Kg/m$^3$] | Specific Heat [J/Kg.K] | Conductivity thermal [W/m.K] |
|---|---|---|---|
| Concrete | 2200 | 880 | 1.5 |

## III.4. Conclusion:

In this chapter, the algorithm of the developed thermal energy storage program is presented.

The studied case is described and the boundary conditions are indicated.

The next chapter contains the results after the execution of the program.

# Chapter IV

# Results and Discussion

## IV.1. Mesh Study

Mesh analysis is preformed in order to reduce numerical calculation errors; the same simulation is repeated for different grid resolution as shown in table

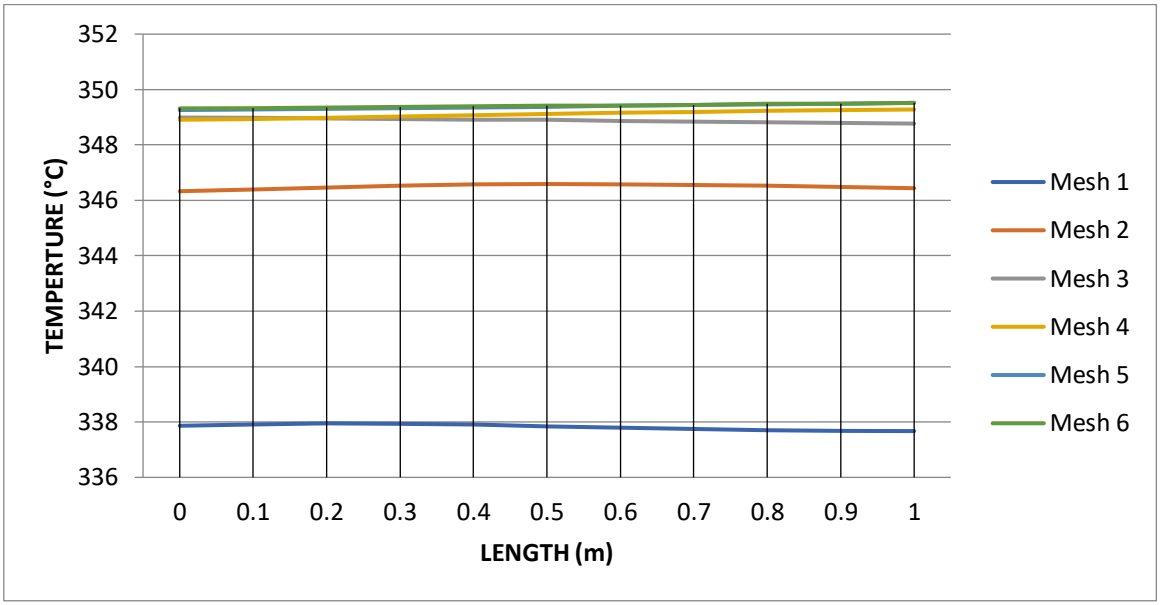


Figure IV- 1: Temperature distribution for different mesh in the line of symmetry.

Table IV-1: Mesh details

| Mesh | Number of nodes | Number of columns | Number of lines | The space dx |
|---|---|---|---|---|
| **01** | **33** | **11** | **3** | **0.1** |
| **02** | **105** | **21** | **5** | **0.05** |
| **03** | **369** | **41** | **9** | **0.025** |
| **04** | **561** | **51** | **11** | **0.02** |
| **05** | **1377** | **81** | **17** | **0.0125** |
| **06** | **3333** | **101** | **33** | **0.00625** |

The figure IV-1 shows that the temperature distribution in the solid varies with the change of the number of nodes. The increase of node number leads the results to converge.

Mesh resolution of 1377 nodes and 3333 nodes don't show any great differences and gives more or less the same result, 1377 node is considered in the program.

### IV.1.1. Optimization of the Battery Using Mode 5.0 Software:

With the help of Modde 5.0 software we intend to optimize the performance of the studied battery. The diameter, velocity of the heat transfer fluid and the spacing between the tubes are considered as variables input of the software, after entering the variables 17 simulations are generated as showen in table IV-2.

Table IV- 2: Simulation generated by the MODDE 5.0 software.

| | 1 | 2 | 3 | 4 | 5 | 6 | 7 |
|---|---|---|---|---|---|---|---|
| | Exp No | Exp Name | Run Order | Incl/Excl | velocity | Diametere | Spacing |
| 1 | 1 | N1 | 6 | Incl | 0.01 | 0.1 | 0.1 |
| 2 | 2 | N2 | 13 | Incl | 0.5 | 0.1 | 0.1 |
| 3 | 3 | N3 | 11 | Incl | 0.01 | 0.2 | 0.1 |
| 4 | 4 | N4 | 10 | Incl | 0.5 | 0.2 | 0.1 |
| 5 | 5 | N5 | 2 | Incl | 0.01 | 0.1 | 0.4 |
| 6 | 6 | N6 | 7 | Incl | 0.5 | 0.1 | 0.4 |
| 7 | 7 | N7 | 15 | Incl | 0.01 | 0.2 | 0.4 |
| 8 | 8 | N8 | 1 | Incl | 0.5 | 0.2 | 0.4 |
| 9 | 9 | N9 | 12 | Incl | 0.01 | 0.15 | 0.25 |
| 10 | 10 | N10 | 16 | Incl | 0.5 | 0.15 | 0.25 |
| 11 | 11 | N11 | 9 | Incl | 0.255 | 0.1 | 0.25 |
| 12 | 12 | N12 | 3 | Incl | 0.255 | 0.2 | 0.25 |
| 13 | 13 | N13 | 8 | Incl | 0.255 | 0.15 | 0.1 |
| 14 | 14 | N14 | 4 | Incl | 0.255 | 0.15 | 0.4 |
| 15 | 15 | N15 | 14 | Incl | 0.255 | 0.15 | 0.25 |
| 16 | 16 | N16 | 5 | Incl | 0.255 | 0.15 | 0.25 |
| 17 | 17 | N17 | 17 | Incl | 0.255 | 0.15 | 0.25 |

After performing the simulations, outlet fluid temperature and battery efficiency are added in to the program as shown in the table IV-3:

Table IV- 3: Data for the simulation with results.

| | 1 | 2 | 3 | 4 | 5 | 6 | 7 | 8 | 9 |
|---|---|---|---|---|---|---|---|---|---|
| | Exp No | Exp Name | Run Order | Incl/Excl | velocity | Diametere | Spacing | Outlet fluid temperature | Effeciency |
| 1 | 1 | N1 | 6 | Incl | 0.01 | 0.1 | 0.1 | 228.422 | 0.86075 |
| 2 | 2 | N2 | 13 | Incl | 0.5 | 0.1 | 0.1 | 239.82 | 0.69497 |
| 3 | 3 | N3 | 11 | Incl | 0.01 | 0.2 | 0.1 | 274.293 | 0.43706 |
| 4 | 4 | N4 | 10 | Incl | 0.5 | 0.2 | 0.1 | 281.095 | 0.28359 |
| 5 | 5 | N5 | 2 | Incl | 0.01 | 0.1 | 0.4 | 303.038 | 0.20715 |
| 6 | 6 | N6 | 7 | Incl | 0.5 | 0.1 | 0.4 | 302.427 | 0.20367 |
| 7 | 7 | N7 | 15 | Incl | 0.01 | 0.2 | 0.4 | 321.1 | 0.10458 |
| 8 | 8 | N8 | 1 | Incl | 0.5 | 0.2 | 0.4 | 311.945 | 0.12834 |
| 9 | 9 | N9 | 12 | Incl | 0.01 | 0.15 | 0.25 | 353.805 | 0.18605 |
| 10 | 10 | N10 | 16 | Incl | 0.5 | 0.15 | 0.25 | 345.2 | 0.1931 |
| 11 | 11 | N11 | 9 | Incl | 0.255 | 0.1 | 0.25 | 330.268 | 0.28493 |
| 12 | 12 | N12 | 3 | Incl | 0.255 | 0.2 | 0.25 | 341.031 | 0.18066 |
| 13 | 13 | N13 | 8 | Incl | 0.255 | 0.15 | 0.1 | 279.536 | 0.42611 |
| 14 | 14 | N14 | 4 | Incl | 0.255 | 0.15 | 0.4 | 319.249 | 0.13012 |
| 15 | 15 | N15 | 14 | Incl | 0.255 | 0.15 | 0.25 | 348.412 | 0.1903 |
| 16 | 16 | N16 | 5 | Incl | 0.255 | 0.15 | 0.25 | 348.412 | 0.1903 |
| 17 | 17 | N17 | 17 | Incl | 0.255 | 0.15 | 0.25 | 348.412 | 0.1903 |

Table IV-4 shows the coefficient list for the outlet fluid temperature:

Table IV- 4: The coefficient list for the outlet fluid temperature.

| | 1 | 2 | 3 | 4 | 5 |
|---|---|---|---|---|---|
| 1 | Outlet fluid temperature | Coeff. SC | Std. Err. | P | Conf. int(±) |
| 2 | Constant | 349.528 | 2.62315 | 3.537e-013 | 6.20285 |
| 3 | vel | -0.0170286 | 1.93857 | 0.993235 | 4.58405 |
| 4 | Dia | 12.5489 | 1.93857 | 0.000342648 | 4.58405 |
| 5 | Spa | 25.4593 | 1.93857 | 3.46291e-006 | 4.58405 |
| 6 | vel*vel | -0.863006 | 3.7452 | 0.824347 | 8.85611 |
| 7 | Dia*Dia | -14.7156 | 3.7452 | 0.00568154 | 8.85611 |
| 8 | Spa*Spa | -50.9727 | 3.7452 | 2.72019e-006 | 8.85611 |
| 9 | vel*Dia | -1.64258 | 2.16739 | 0.473269 | 5.12512 |
| 10 | vel*Spa | -3.49576 | 2.16739 | 0.150803 | 5.12512 |
| 11 | Dia*Spa | -7.4457 | 2.16739 | 0.010906 | 5.12512 |
| 12 | | | | | |
| 13 | N = 17 | Q2 = | 0.910 | Cond. no. = | 4.4382 |
| 14 | DF = 7 | R2 = | 0.989 | Y-miss = | 0 |
| 15 | | R2 Adj. = | 0.975 | RSD = | 6.1303 |
| 16 | | | | Conf. lev. = | 0.95 |

The coefficient list for the outlet fluid temperature in form of a histogram graph help to determent the main factors that impact the results.

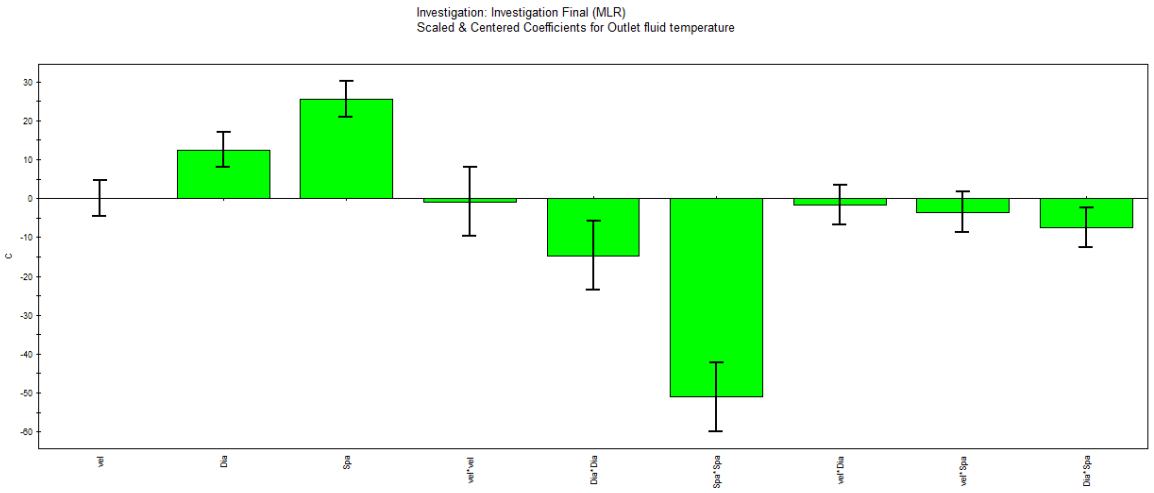


Figure IV- 2: The coefficient graph for the outlet fluid temperature.

Figure IV-2 shows all the factors, the ones that have a significant impact should be considered.

The table IV-5 shows the efficiency coefficient list:

Table IV- 5: The coefficient list for the efficiency.

| | 1 | 2 | 3 | 4 | 5 |
|---|---|---|---|---|---|
| 1 | **Effeciency** | **Coeff. SC** | **Std. Err.** | **P** | **Conf. int(±)** |
| 2 | **Constant** | 0.18013 | 0.0212737 | 6.33251e-005 | 0.0503049 |
| 3 | **vel** | -0.029192 | 0.0157217 | 0.105707 | 0.0371764 |
| 4 | **Dia** | -0.111724 | 0.0157217 | 0.000192585 | 0.0371764 |
| 5 | **Spa** | -0.192862 | 0.0157217 | 5.48384e-006 | 0.0371764 |
| 6 | **vel*vel** | 0.0170722 | 0.0303734 | 0.591597 | 0.0718226 |
| 7 | **Dia*Dia** | 0.0602923 | 0.0303734 | 0.0875296 | 0.0718226 |
| 8 | **Spa*Spa** | 0.105612 | 0.0303734 | 0.0103061 | 0.0718226 |
| 9 | **vel*Dia** | 0.00494377 | 0.0175774 | 0.786646 | 0.0415645 |
| 10 | **vel*Spa** | 0.0424413 | 0.0175774 | 0.0464634 | 0.0415645 |
| 11 | **Dia*Spa** | 0.0821463 | 0.0175774 | 0.00227838 | 0.0415645 |
| 12 | | | | | |
| 13 | N = 17 | Q2 = | 0.800 | Cond. no. = | 4.4382 |
| 14 | DF = 7 | R2 = | 0.975 | Y-miss = | 0 |
| 15 | | R2 Adj. = | 0.943 | RSD = | 0.0497 |
| 16 | | | | Conf. lev. = | 0.95 |

The table IV-5 shows the entire coefficient list that can help determine the main factors that has major impact on the results of the efficiency.

After 5000 iteration the optimal parameters according to the software are shown below in table IV-6:

Table IV- 6: Optimization result.

Iteration: 5004 Iteration slider:

| | 1 | 2 | 3 | 4 | 5 | 6 | 7 |
|---|---|---|---|---|---|---|---|
| | velocity | Diametere | Spacing | Outlet fluid temperature | Effeciency | iter | log(D) |
| 1 | 0.01 | 0.1 | 0.1086 | 240.189 | 0.7964 | 5001 | 1.6883 |
| 2 | 0.01 | 0.143 | 0.2425 | 344.771 | 0.2566 | 5001 | 1.539 |
| 3 | 0.0114 | 0.1 | 0.13 | 258.066 | 0.7243 | 5001 | 1.56 |
| 4 | 0.01 | 0.1599 | 0.2238 | 344.552 | 0.2472 | 5000 | 1.5524 |
| 5 | 0.01 | 0.143 | 0.2425 | 344.778 | 0.2565 | 5000 | 1.5391 |
| 6 | 0.01 | 0.1429 | 0.2427 | 344.775 | 0.2566 | 5004 | 1.539 |
| 7 | 0.01 | 0.143 | 0.2425 | 344.778 | 0.2565 | 5000 | 1.5391 |
| 8 | 0.01 | 0.143 | 0.2425 | 344.778 | 0.2565 | 5000 | 1.5391 |

So the optimal parameters of the battery are a fluid velocity of 0.01m/s, tube diameter of 0.143m and spacing between tubes of 0.2425m.

Also these simulations were done at vapor mass flow of 0.00004kg/s for each tube.

## IV.2. Fluid Temperature

### IV.2.1. Fluid Temperature at Charging Phase

#### a. One meter (1m) length:

Fluid temperature at charging phase at both inlet and outlet in 1m long batteryis presented in figure IV-3.

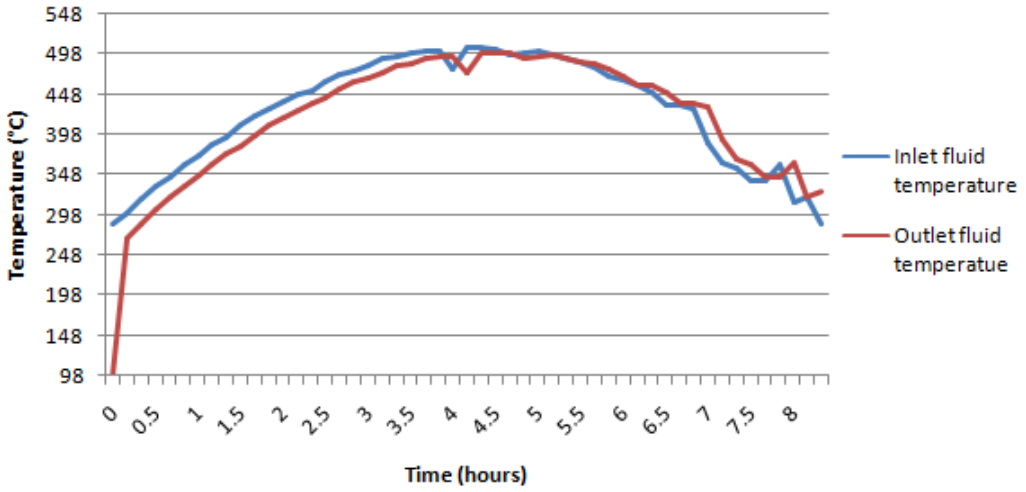


Figure IV- 3: Inlet and outlet fluid temperature in 1 meter long battery.

The results obtained show the fluid temperature at inlet and outlet in a period of 8 hours and 20 minutes.

The inlet fluid temperature began from 287°C, it continues to increases until it reached a peak temperature of 503.39°C. It started to decrease reaching temperature of a 287°C at the end. While the outlet fluid temperature began from 98°C which is the battery's initial temperature, increases to 499.8°C after 4 hours and 30 minutes then decreases to 326.39°C at the end.

**b. Ten meter (10m) length:**

Fluid temperature at charging phase at both inlet and outlet in 10m long battery is presented in figure IV-4.

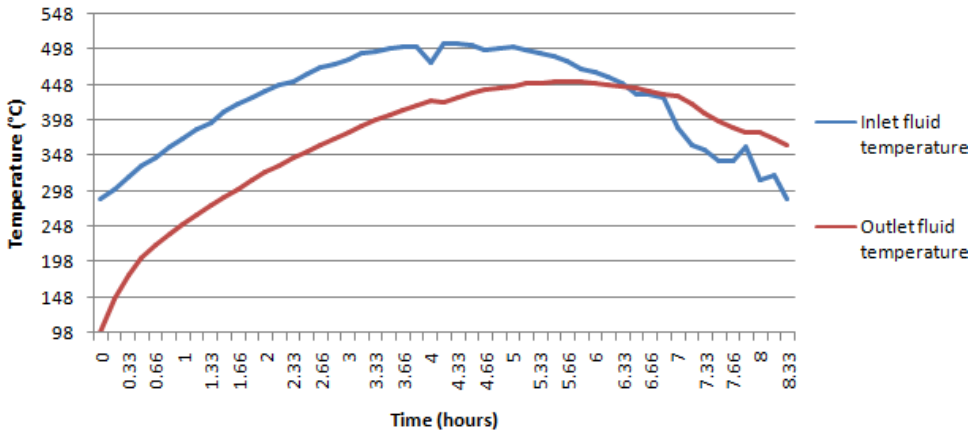


Figure IV- 4: Inlet and outlet fluid temperature in 10 meter long battery at charging phase.

The results obtained, figure IV-4, show the fluid temperature at inlet and outlet in a period of 8 hours and 20 minutes.

The inlet fluid temperature began from 287°C, it continues to increases until it reached a peak temperature of 503.39°C. It started to decrease reaching temperature of a 287°C at the end. While the outlet fluid temperature began from 98°C which is the battery's initial temperature, increases to 453.8°C after 6 hours then decreases to 358.47°C at the end. After the point where the tow graphs cross each other there might be cooling of the battery.

### IV.2.2. Fluid Temperature at Discharging Phase

**a. One meter (1m) length:**

Fluid temperature at discharging phase at inlet and outlet in 1m long battery is presented in figure IV-5.

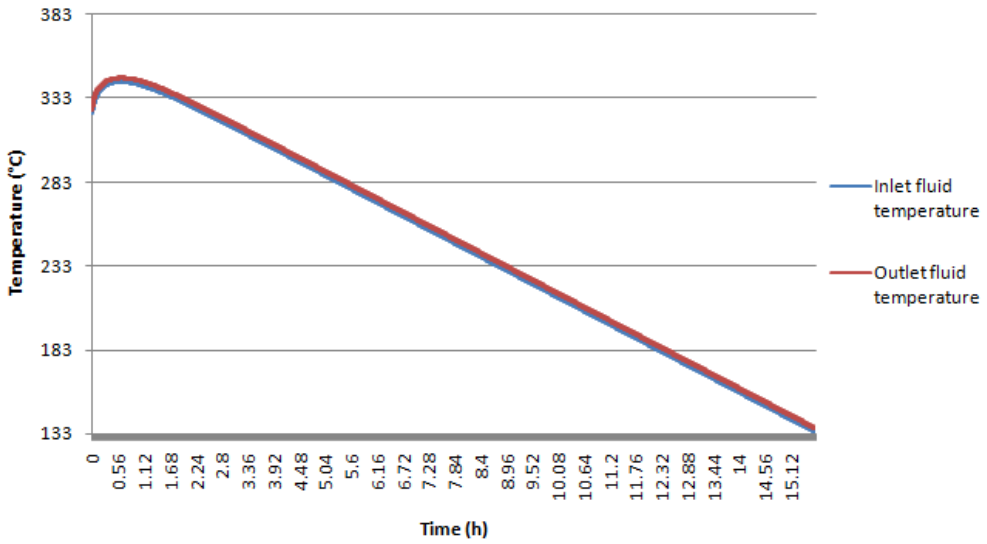


Figure IV- 5: Inlet and outlet fluid temperature in 1 meter long battery at discharging phase.

The first graph is labeled inlet fluid temperature while the second is labeled outlet fluid temperature.

Both graphs clearly show a consistent decrease in temperature over time. In the first graph (inlet fluid temperature), temperature begin at 324.08°C then increases to 342.85°C, gradually decline until reaching their lowest point which is 133.93°C. The second graph (outlet fluid temperature) exhibits a similar pattern, with temperature peaking of 345.13°C and then steadily declining until reaching a minimum temperature of 136.54°C.

**b. Ten meter (10m) length:**

Fluid temperature at both inlet and outlet in 10m long battery at discharging phase is presented in figure IV-6.

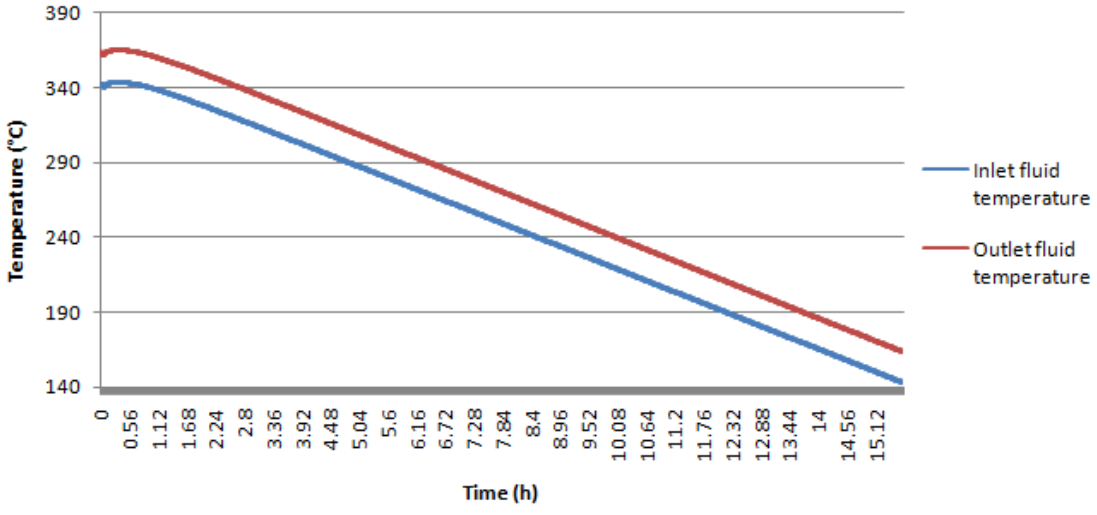


Figure IV- 6 Inlet and outlet fluid temperature in 10 meter long battery at discharging phase.

The first graph is labeled inlet fluid temperature while the second is labeled outlet fluid temperature.

Both graphs clearly show a consistent decrease in temperature over time. In the first graph (inlet fluid temperature), temperature begin at 342.43°C, gradually decline until reaching their lowest point which is 142.99°C. The second graph (outlet fluid temperature) exhibits a similar pattern, with temperature peaking of 363.90°C and then steadily declining until reaching a minimum temperature of 163.41°C.

## IV.3. Solid Temperature

### A. Solid Temperature 1m Long Battery:

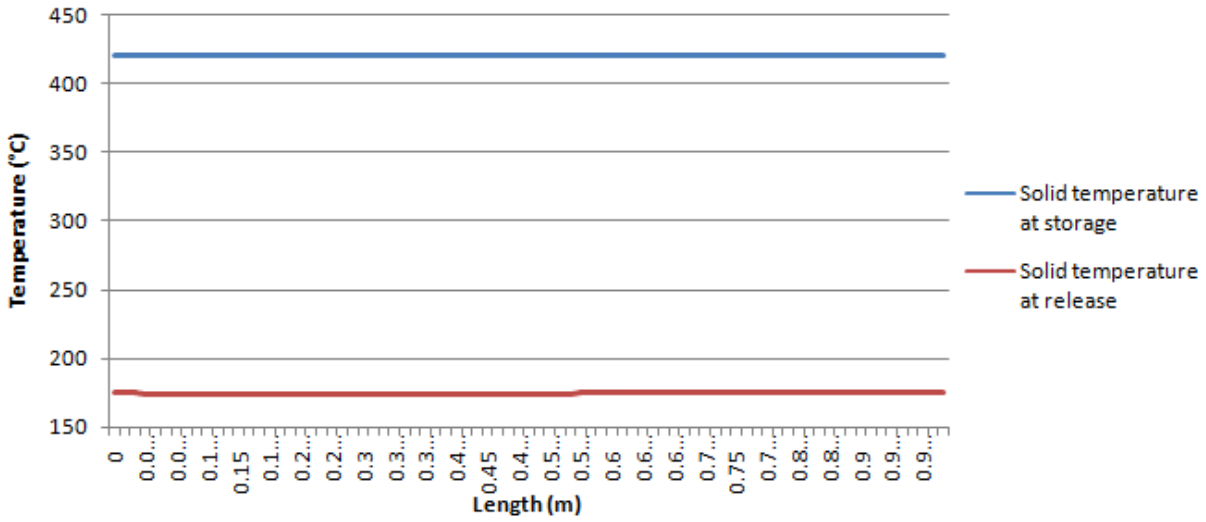


Figure IV- 7: Solid temperature in 1 meter long battery symmetry line.

Figure IV-7 shows the solid temperature in symmetry line at the end of each cycle.

### B. Solid Temperature in 10m Long Battery:

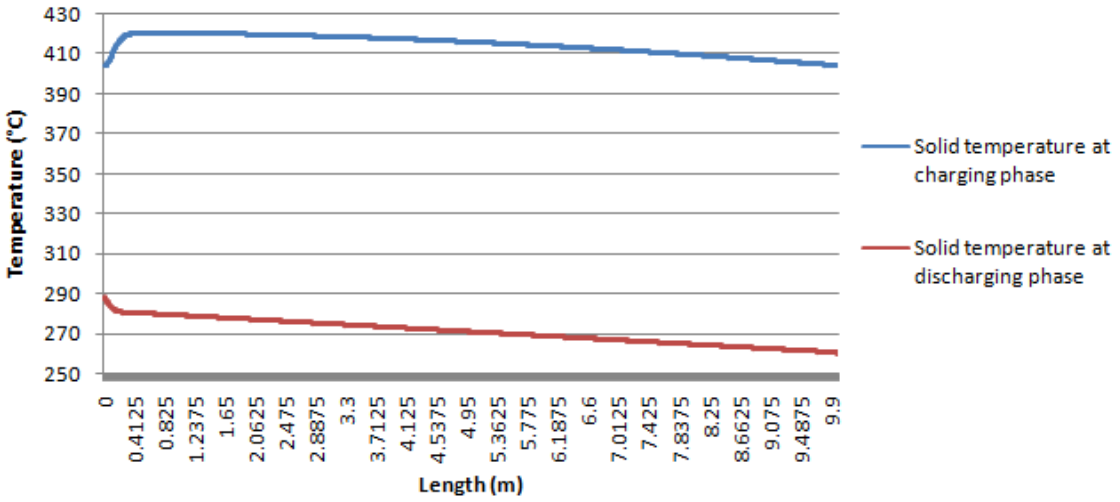


Figure IV- 8: Solid temperature at in 10 meter long battery symmetry line.

Figure IV-8 shows the solid temperature in symmetry line at the end of each cycle.

The main difference between the 1m and 10m batteries is the battery temperature at discharging phase is much higher than the 1m battery.

## IV.4. Comparison between the Fluid Temperatures at Outlet

### IV.4.1. Charging Phase

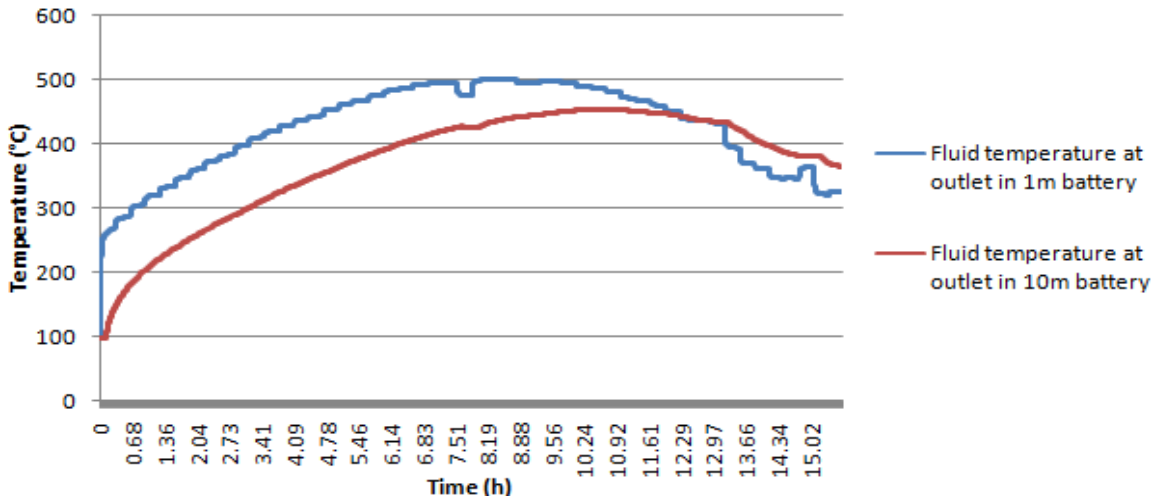


Figure IV- 9: Fluid temperature at outlet in charging phase.

The difference of the fluid temperature at outlet between the two batteries is presented in figure IV-9. 1m long batteries can charge rapidly while the 10m long battery charge slowly but hold more energy and releases fluid at higher temperature.

### IV.4.2. Discharging Phase:

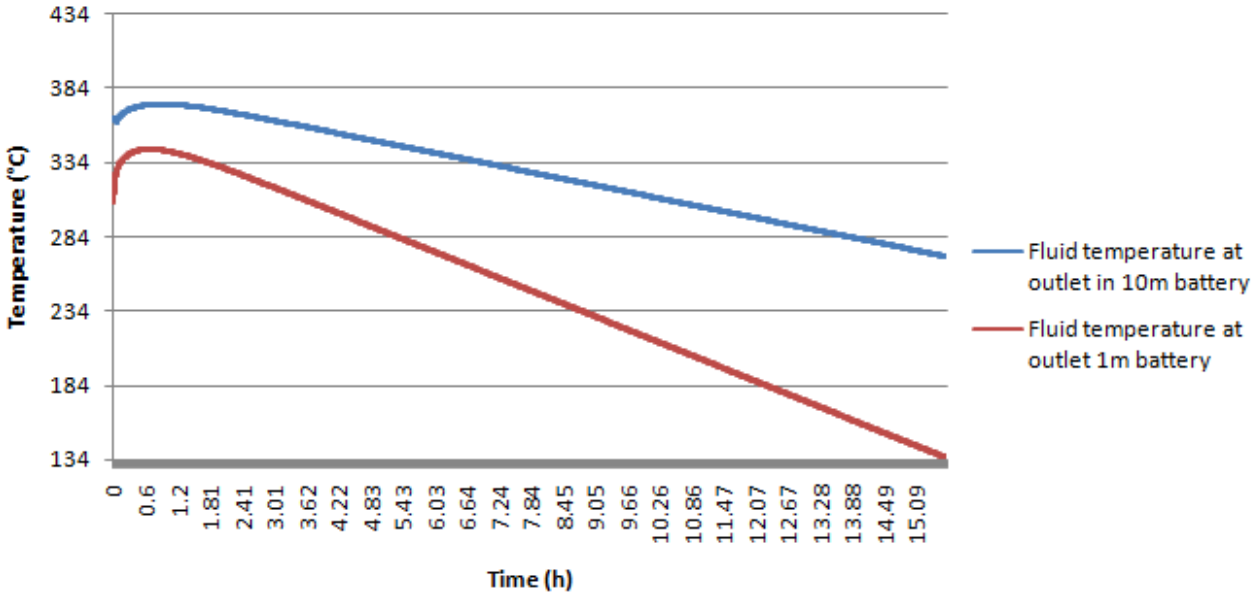


Figure IV- 10: Fluid temperature at outlet in discharging phase.

The difference of the outlet fluid temperature between the 1 and 10m batteries is shown in figure IV-10. The 1m long batteries discharge rapidly while the 10m long battery discharges slowly because of the energy capacity he could hold also releases fluid at higher temperature.

## IV.5. Conclusion:

This chapter deals with the results obtained from numerical simulation of battery in storage and release phases.

First of all, we carried out a mesh study to minimize computational errors. Secondly, we optimized the parameters of the battery by changing velocity, distance between tubes, and tube diameter.

# CONCLUSION

## Conclusion

Thermal energy can be stored as sensible heat in solids. This type of storage allows the highest possible storage temperature levels, avoiding the problem of high vapor pressure in liquid environments.

The literature was studied, including recent developments and works in the field of parabolic trough concentrated solar energy (CSP) and thermal energy storage.

This study presents a numerical simulation of a thermal energy storage system using concrete as the storage environment and liquid sodium as the heat transfer fluid.

The simulation of the conduction equation is solved by the finite-difference method using the explicit scheme.

Using Modde 5 software the optimum parameters of the battery are a heat transfer fluid velocity in both charging phase and discharging of 0.01 m/s, tube diameter tube diameter of 0.143 m, tube spacing of 0.121 m and battery length of 10 m.

# REFERENCES

# References


[1] Hussein A. Mohammed, Hari B. Vuthaluru, Shaomin Liu, Parabolic Trough Solar Collectors: Thermal and Hydraulic Enhancement Using Passive Techniques and Nanofluids, 29 October 2022, 1st Edition, Springer Cham, ISBN: 978-3-031-08700-4, https://doi.org/10.1007/978-3-031-08701-1

[2] H.Ö. Paksoy, B. Beyhan, (2015). Thermal energy storage (TES) systems for greenhouse technology : Advances in Thermal Energy Storage Systems, Methods and Applications Woodhead Publishing Series in Energy, Pages 533-548 , https://doi.org/10.1533/9781782420965.4.533.

[3] Sergii Bespalko, Alberto Munoz Miranda, Oleksii Halychyi.(2018),OVERVIEW OF THE EXISTING HEAT STORAGE TECHNOLOGIES, SENSIBLE HEAT, RIC Pro-Akademia, ISSN 2300-5599 , https://doi.org/10.32933/ActaInnovations.28.8.

[4] C. Guan, H. Lu, L. Zhang et al. (2020), Regulation of the output temperature in a novel water heating system using solid graphite as sensible heat thermal energy storage medium: Effects of water tank, Energy Reports 6 160–171, https://doi.org/10.1016/j.egyr.2020.06.006

[5] Sarbu Ioan, Calin Sebarchievici.(2018),A Comprehensive Review of Thermal Energy Storage,Department of Building Services Engineering, Polytechnic University of Timisoara, **https://doi.org/10.3390/su10010191**.

[6] Schumann, T.E.W. (1929), Heat Transfer: A Liquid Flowing through a Porous PrismJournal of the Franklin Institute Volume 208, Issue 3, Pages 405-416 , https://doi.org/10.1016/S0016-0032(29)91186-8

[7] Ryan Anderson, Liana Bates, Erick Johnson, Jeffrey F Morris.(2015), Packed bed thermal energy storage: A simplified experimentally validated model, Journal of Energy Storage 4:14 , https://doi.org/10.1016/j.est.2015.08.007.

[8] Panna Lal Singh.(2015), **Thermal performance of packed bed heat storage system for solar air heaters**, Energy for Sustainable Development Volume 29 , Pages 112-117 , https://doi.org/10.1016/j.esd.2015.10.010

[9] Magdalena Nemś, Artur Nemś, Jacek Kasperski, Michał Pomorski.(2017), Thermo-Hydraulic Analysis of Heat Storage Filled with the Ceramic Bricks Dedicated to the Solar Air Heating System, Faculty of Mechanical and Power Engineering, Wroclaw University of Science and Technology, https://doi.org/10.3390/ma10080940

[10] Yongfang Jian,Quentin Falcoz, Pierre Neveu, Fengwu Bai, Yan Wang, Zhifeng Wang, Design and optimization of solid thermal energy storage modules for solar thermal power plant applications , Applied Energy Volume 139, 1 February 2015, Pages 30-42, https://doi.org/10.1016/j.apenergy.2014.11.019.

[11] Abdul Jabbar N. Khalifa, Ehsan F. Abbas, **A comparative performance study of some thermal storage materials used for solar space heating**, Energy and Buildings Volume 41, Issue 4, April 2009, Pages 407-415 , https://doi.org/10.1016/j.enbuild.2008.11.005.

[12] Messaoud Sandali,Abdelghani Boubekri,Djamel Mennouche, (2018), Thermal behavior modeling of a cabinet direct solar dryer as influenced by sensible heat storage in a fractured porous medium, *AIP Conf. Proc*. 1968, 0200148, https://doi.org/10.1063/1.5039173.

[13] Niyas. H, Prasad. L, Muthukumar. P. (2014) , Performance investigation of high-temperature sensible heat thermal energy storage system during charging and discharging cycles. Clean Technologies and Environmental Policy, 17, 501-513, DOI: 10.1007/s10098-014-0807-7

[14] Burcu. Koçak, Ana.Ines. Fernandez, Halime. Paksoy .(2020), **Review on sensible thermal energy storage for industrial solar applications and sustainability aspects**, Solar Energy Volume 209, Pages 135-169, https://doi.org/10.1016/j.solener.2020.08.081

[15] CHEKABA Aimad, Bouguerra Amina, (2020), Simulation numérique du stockage d'énergie solaire thermique d'une installation thermodynamique; ELM-16/01, https://docplayer.fr/212806327-Liste-des-memoires-de-fin-d-etudes-pour-l-obtention-de-master-departement-elm.html

[16] E. C. F. Koumad. A. (2021). " Etude d'un élément de stockage de l'énergie thermique ".

[17] E. C. F Rahal. A and Khalifa med. A Koumad. A. (2021). " Élaboration d'un Logiciel de Calcul de Stockage d'Energie Thermique Sensible".

[18] Andrea Giostri, Marco Binotti, Marco Astolfi, Paolo Silva, Ennio Macchi, Giampaolo Manzolini, **Comparison of different solar plants based on parabolic trough technology,** Solar Energy Volume 86, Issue 5, May 2012, Pages 1208-1221, https://doi.org/10.1016/j.solener.2012.01.014.

[19] SUVI SUOJANEN, (2016), Development of concentrated solar power and conventional power plant hybrids Tampere University of technology Master of Science Thesis, 140 pages, 13 Appendix pages, https://urn.fi/URN:NBN:fi:tty-201602153521.

[20] H.G. Jin, H. Hong, (2012), **Hybridization of concentrating solar power (CSP) with fossil fuel power plants**, Concentrating Solar Power Technology Principles, Developments and Applications Woodhead Publishing Series in Energy, Pages 395-420, https://doi.org/10.1533/9780857096173.2.395

[21] H.M.I. Pousinho, J. Contreras, P. Pinson, V.M.F. Mendes,(2015), **Robust optimisation for self-scheduling and bidding strategies of hybrid CSP–fossil power plants**, International Journal of Electrical Power & Energy Systems,Volume 67, Pages 639-650, https://doi.org/10.1016/j.ijepes.2014.12.052

[22] David Barlev, Ruxandra Vidu, Pieter Stroeve, (2011), **Innovation in concentrated solar power**, Solar Energy Materials and Solar Cells,Volume 95, Issue 10, Pages 2703-2725,https://doi.org/10.1016/j.solmat.2011.05.020

[23] Soteris A. Kalogirou,(2014), Chapter 10 - **Solar Thermal Power Systems**, Solar Energy Engineering (Second Edition),Processes and Systems, Pages 541-581,https://doi.org/10.1016/B978-0-12-397270-5.00010-8

[24] Isabel Llorente García, José Luis Álvarez, Daniel Blanco,(2011), **Performance model for parabolic trough solar thermal power plants with thermal storage: Comparison to operating plant data**, Solar Energy,Volume 85, Issue 10, Pages 2443-2460,

https://doi.org/10.1016/j.solener.2011.07.002

[25] AIE International Energy Agency, (2015), Technology Roadmap Solar Thermal Electricity, IEA Technology Roadmaps, Éditions OCDE Paris, https://doi.org/10.1787/9789264238824-en.

[26] RAFAEL GUÉDEZ,(2016), A Techno-Economic Framework for the Analysis of Concentrating Solar Power Plants with Storage, Doctoral Thesis, 2016 KTH Royal Institute of Technology Industrial Engineering and Management Department of Energy Technology Heat and Power Division SE-100 44, Stockholm, Sweden, ISBN: 978-91-7729-086-5, https://www.diva-portal.org/smash/get/diva2:956167/FULLTEXT01.pdf

[27] Matthias Günther , (2011), Chapter 6, Linear Fresnel Technology, Advanced CSP Teaching Materials, https://dokumen.tips/documents/chapter-6-linear-fresnel-technology-energy-energy-figure-5-solarmundo-fresnel.html?page=1.

[28] Matthias Günther,Michael Joemann,Simon Csambo,(2011), Chapter 5 Parabolic Trough Technology, Advanced CSP Teaching Materials, https://docplayer.net/32427036-Chapter-5-parabolic-trough-technology.html.

[29] E. Zarza Moya,(2012), Parabolic-trough concentrating solar power (CSP) systems, Concentrating Solar Power Technology, Principles, Developments and Applications Woodhead Publishing Series in Energy, Pages 197-239, https://doi.org/10.1533/9780857096173.2.197.

[30] Ibrahim Dincer,(2002),**On thermal energy storage systems and applications in buildings**, Energy and Buildings,Volume 34.Issue 4.Pages 377-388,https://doi.org/10.1016/S0378-7788(01)00126-8.

[31] Dr. Stefan Oberholze,(2021),Technologies de stockage de l'énergie, Office fédéral de l'énergie OFEN,file:///C:/Users/Lenovo/Downloads/106232021.09.06_Stockage%20de%20l'%C3%A9nergie_Synth%C3%A8se.pdf.

[32] S. Kalaiselvam, R. Parameshwaran,(2014), **Sensible Thermal Energy Storage**, Thermal Energy Storage Technologies for Sustainability,Systems Design, Assessment and Applications,, Pages 65-81, https://doi.org/10.1016/B978-0-12-417291-3.00004-9.

[33] Marc Medrano, Antoni Gil, Ingrid Martorell, Xavi Potau, Luisa F. Cabeza,(2010), **State of the art on high-temperature thermal energy storage for power generation. Part 2—Case studies**, Renewable and Sustainable Energy Reviews,Volume 14, Issue 1, Pages 56-72,https://doi.org/10.1016/j.rser.2009.07.036.

[34] Antoni Gil, Marc Medrano, Ingrid Martorell, Ana Lázaro, Pablo Dolado, Belén Zalba, Luisa F. Cabeza,2010, **State of the art on high temperature thermal energy storage for power generation. Part 1-Concepts, materials and modellization**, Renewable and Sustainable Energy Reviews,Volume 14, Issue 1, Pages 31-55,https://doi.org/10.1016/j.rser.2009.07.035.

[35] Dr. Yilma.T,(2020),computational heat transfer, EXPLICIT FINITE DIFFERENCE METHOD [STEADY STATE CONDITION,http://ndl.ethernet.edu.et/bitstream/123456789/87833/1/Chapter%201%20Lecture.pdf.

[36] THEODORE.L.BERGMAN, ADRIENNE.S.LAVINE, FRANK.P. INCROPERA, DAVID.P.DEWITT,,Fundamentals of Heat and Mass Transfer, SEVENTH EDITION,16 May 2011,pages706-730, ISBN 13 978-0470-50197-9,https://mech.at.ua/HeatandMassTransfer7thEdition-Incropera-dewitt.pdf.

# ANNEXES

# Annexes

## Liquid sodium properties

| Temperature(c) | Density (kg/m$^3$ ) | Specific heat (J/kg) | Thermal conductivity (W/m.K) | Dynamic viscosity(pa.s) |
|---|---|---|---|---|
| **98** | **926** | **1383** | **89.44** | **6.88** |
| **127** | **919** | **1372** | **87.22** | **5.99** |
| **227** | **897** | **1334** | **80.09** | **4.15** |
| **427** | **874** | **1301** | **73.70** | **3.21** |
| **527** | **852** | **1277** | **68.00** | **2.64** |
| **627** | **828** | **1260** | **62.90** | **2.27** |
| **727** | **805** | **1252** | **58.34** | **2.01** |